行政院所屬各機關因公出國人員出國報告書
（出國類別：其他）

參加第 51 屆美國國家海洋暨大氣總署全球監測年會(NOAA/GML 51st Global Monitoring Annual Conference)

服務機關：行政院環境保護署
姓名職稱：黃健瑋環境監測技術師
派赴國家：美國
出國期間：112 年 5 月 21 日至 5 月 27 日
報告日期：112 年 8 月 18 日

摘要

本署鹿林山大氣背景測站為東亞大氣污染長程傳輸之中繼站，反映氣候變遷及污染物長期趨勢變化，並持續推動國際空氣品質監測國際合作，為與美國國家海洋暨大氣總署(NOAA/GML)交流監測技術與成果，於 2023 年 5 月 23 日至 24 日(美國時間)出席第 51 屆美國國家海洋暨大氣總署全球監測年會(NOAA/GML 51st Global Monitoring Annual Conference)，會議地點為美國科羅拉多州波德(Boulder, CO)。

本次年會主要由美國及加拿大等國家，包含美國國家海洋暨大氣總署(NOAA)、美國國家航空暨太空總署(NASA)及各學術研究人員與會，包含口頭報告及論文發表兩部份。口頭報告分為「碳循環與溫室氣體」「鹵碳化合物與高層大氣觀測」「輻射與氣膠」及「空氣品質」等四大主題、計 36 個子題目，並有 42 篇論文海報展示。其中本署與國立中央大學共同進行「東亞鹿林山氣膠濃度與太陽輻射之長期研究」口頭報告，並發表「溫室氣體在南海的碳循環變化」與「副熱帶東亞自由對流層的氣團起源：鹿林山大氣背景站後推軌跡分析」2 篇論文海報。

此外，本次另安排拜訪加州空氣資源局(California Air Resources Board, CARB)許英光博士，針對美國目前對於溫室氣體監測進行瞭解及相關討論，包含目前衛星觀測應用與其優缺點、適合於我國地理環境之監測方法及測量結果、技術等如何與溫室氣體減排法規結合等，可作為本署後續相關業務規劃之參考。

目錄

壹、 目的及背景說明

一、 美國國家海洋暨大氣總署全球監測實驗室(NOAA Global Monitoring Laboratory, GML)

美國國家海洋暨大氣總署全球監測實驗室 (NOAA Global Monitoring Laboratory, GML) 研究旨在解決「溫室氣體和碳循環的反饋」、「雲、氣膠和地表輻射的變化」及「平流層臭氧的恢復」，以能夠理解變化原因和結果的方式，取得、評估和提供大氣氣體、氣膠顆粒、雲和地表輻射的長期且準確紀錄。

研究目標為運作關鍵的大氣變量參考觀測系統，包含長期溫室氣體、水蒸氣、臭氧、臭氧消耗物質、氣膠、輻射和雲，並發展新的大氣觀測、分析和建立模型能力，以理解對過去和未來變化的過程。半個世紀以來，透過觀測網路、測量技術和分析工具不斷的發展，確保盡可能產出有效且嚴謹的資訊。另維護校準系統並提供校準服務，以支持世界氣象組織的全球大氣監測計劃。

二、 會議目的

本署鹿林山大氣背景測站為東亞大氣污染長程傳輸之中繼站，反映氣候變遷及污染物長期趨勢變化，並持續推動國際空氣品質監測國際合作，其中美國國家海洋暨大氣總署(NOAA)為重要合作夥伴之一。

美國國家海洋暨大氣總署全球監測實驗室 (NOAA Global Monitoring Laboratory, GML)持續辦理全球監測年會，旨在不斷了解有關微量氣體、氣膠、輻射、臭氧和氣候驅動力等最新觀測結果，並提供一個可以轉發和討論這些觀測結果的論壇，除 NOAA/GML 的監測和研究結果過去一年的，並有其他國家和國際計畫的獨立和合作研究人員的口頭報告和海報展示，以展示最新觀測、分析和建模等方面的新發現和突破性成果。

貳、 會議行程說明

此次行程始於 2023 年 5 月 21 日上午，由臺灣啟程飛往美國加州舊金山(San Francisco, CA)，再前往加州沙加緬度 (Sacramento, CA) ，於 5 月 22 日（美國當地時間）拜訪加州空氣資源局(California Air Resources Board, CARB)許英光博士，針對溫室氣體監測進行相關討論，隨後搭機前往科羅拉多州丹佛(Denver, CO)，並前往會議所在地波德(Boulder, CO)。

5 月 23 日（美國當地時間）於美國科羅拉多大學波德分校(University of Colorado Boulder, CU Boulder)展開第 51 屆美國國家海洋暨大氣總署全球監測年會(NOAA/GML 51st Global Monitoring Annual Conference)。開幕首先由 NOAA 全球監測實驗室(NOAA Global Monitoring Laboratory, GML)主任 Vanda Grubišić 博士致詞，後續分為 2 個主題及海報展示討論，包含「鹵碳化合物與高層大氣觀測(1)」及「碳循環與溫室氣體(1)」等主題，計 12 個報告；另計有 42 篇論文海報，其中包含本署與國立中央大學共同發表「溫室氣體在南海的碳循環變化」及「副熱帶東亞自由對離層的氣團起源：鹿林山大氣背景站後推軌跡分析」等 2 篇論文海報。

5 月 23 日（美國當地時間）持續進行四個主題報告，包含「輻射與氣膠」「鹵碳化合物與高層大氣觀測(2)」「空氣品質」及「碳循環與溫室氣體(2)」，共計有 24 個報告，其中包含本署與國立中央大學共同發表「東亞鹿林山氣膠濃度與太陽輻射之長期研究」，並由國立中央大學黃翔昱博士進行口頭報告。

參、 會議內容及成果說明

一、 拜訪加州空氣資源局(California Air Resources Board, CARB)許英光博士

(一) CRAB 與美國國家航空暨太空總署噴射推進實驗室(NASA Jet Propulsion Laboratory, JPL)在今(2023)年合作發射 2 顆甲烷衛星，除了用於監控石油、天然氣洩漏外，因美國畜牧業發達，也致力於量化乳製品中的甲烷(CH_4)含量，臺灣可考慮應用於垃圾掩埋場，或是污水處理廠可能排放的甲烷(CH_4)、氧化亞氮(N_2O)及有害空氣污染物等，但該衛星目前僅有美國的數據。

(二) CARB 透過衛星或與 Carbon Mapper 合作利用機載遙測光譜儀，主要工作在於探測廢棄油/氣井，因許多油/氣井洩漏已達可能發生爆炸的情況，需要做封存，而需注意衛星僅能監測到大量的甲烷(CH_4)排放源，若相對較小的排放源但加總起來夠大量也可以。因此，對衛星來說仍有許多「不可見」的小排放源，如去(2022)年加州 Bakersfield 一個新興社區，有民眾散步時發現有氣體聲，經確認該社區是建立在廢棄的油/氣井之上，因沒有正確封蓋，使該社區甲烷(CH_4)濃度洩漏已達可能爆炸情況，但因總體排放量仍未達到衛星遙測可發現的程度，只能另使用氣體分析儀進行檢測。

(三) CARB 發射甲烷衛星是由匿名的富人資助，對臺灣可能較不可行，因此建議可參考機載觀測，如 JPL 研究員已研發出小型中紅外線甲烷感測器(Methane Mid-IR Sensor)，可裝載於大型無人機(UAV)上進行監測，但該感測器目前尚未找到廠商可承接技術移轉，故還未能量產。另普林斯頓大學(Princeton University)亦有教授進行相關實驗，而其所使用僅為市售、商用感測器。如對機載觀測有興趣，後續可協助安排與 JPL

研究員進行會議討論。

(四) CARB 的溫室氣體監測網，其用於量化區域尺度的排放量，只能看到整體的排放及追蹤長期趨勢，無法了解個別的來源。如臺灣也想建立溫室氣體監測網，測站選址首要同空氣品質監測站，需考量如氣象條件（風向）、污染物濃度分布等，但更重要的是要確認鄰近測站無局部的污染源影響，否則可能讓監測數據失真，設站地點建議可選在污染源下風處且地勢較高的地方。

(五) 為了驗證溫室氣體排放量和減排計劃，需要有一個可靠且合理的排放清單，以此為基礎來驗證何時達法規規定的目標。因此，根據環境空氣監測來量化排放量並找出洩漏的物種和數量，如 CARB 在 Mt. Wilson 發現甲烷(CH_4)被低估了 30%，直到與加州理工學院(California Institute of Technology)教授及美國國家海洋暨大氣總署(NOAA)合作，透過甲烷/乙烷比率，才了解被低估的甲烷(CH_4)來自天然氣管道，也因此才能夠更新排放因子並改進排放清單。另目前也與加州理工學院合作嘗試以同位素來驗證二氧化碳(CO_2)排放量，因其是最主要的溫室氣體，一旦得到驗證，即可以根據排放量來訂定相關法規。

二、 參加第 51 屆美國國家海洋暨大氣總署全球監測年會 (NOAA/GML 51st Global Monitoring Annual Conference)

(一) 中國的四氟甲烷(CF_4)和六氟乙烷(C_2F_6)排放增加量與全球相比是為持平或更大，對全球排放的貢獻正在增加。而中國西部地區的鋁相關工業是四氟甲烷(CF_4)和六氟乙烷(C_2F_6)主要排放來源，如四氟甲烷(CF_4)與鋁工業更有關聯；六氟乙烷(C_2F_6)則是與鋁工業及半導體工業有關。

(二) 由於大氣中的甲烷(CH_4)快速增加，全球承諾至 2030 年排放量

要減少 30%，為達此目標應先瞭解大氣中甲烷(CH_4)的增長過程，包含區分化學、自然及人為的貢獻。美國國家海洋暨大氣總署(NOAA)已可利用甲烷(CH_4)的 ^{13}C 穩定同位素測量及區分化石燃料和微生物來源之間的排放，這些量測顯示最近大氣中的甲烷(CH_4)增加主要由微生物來源主導，可能來自人為和自然來源的組合，並已觀察到在熱帶和北半球高緯度地區，大氣中的甲烷(CH_4)是如何增長。

(三) 隨著氣候變化變得更加嚴重，許多國家承諾到本世紀中期達成碳中和，就須利用各種方法觀測二氧化碳(CO_2)來提高對化石燃料排放和自然碳通量的理解，因此，量化區域碳通量以支持減碳政策至關重要。二氧化碳(CO_2)觀測可分為衛星、機載及地面觀測，衛星具有覆蓋全球的優勢，但容易出現偏差；地面觀測較準確，但空間覆蓋範圍有限；機載觀測在時間和空間上有其限制，但提供了地面和衛星觀測所缺乏的垂直觀測資訊。未來應更加利用衛星、地面和機載觀測的互補特徵，將化石燃料排放與自然碳通量估算相結合。

(四) 2020 年韓國國家環境研究院(National Institute of Environmental Research of the Korean Ministry of Environment)發射 GEO-KOMPSAT 2B 衛星，並搭載地球同步環境監測光譜儀(Geostationary Environment Monitoring Spectrometer, GEMS)，由原每天僅有一次通過觀測地區的低軌道繞極衛星，進入了地球同步觀測空氣品質的新時代，目前 GEMS 已經對東亞地區進行 2.5 年的空氣品質監測。美國國家航空暨太空總署(NASA)也在今(2023)年 4 月發射「監控對流層排放的空氣污染物」儀器(Tropospheric Emissions: Monitoring of Pollution, TEMPO)，將自夏天起對北美地區提供地球同步空氣品質監測。美國國家海洋暨大氣總署(NOAA)

也將發展地球同步擴展觀測計畫(Geostationary Extended Observations mission, GeoXO)，預計於 2036 年發射搭載大氣成分儀器(Atmospheric Composition Instrument, ACX)衛星。地球同步空氣品質觀測，可提供零星及快速變化排放源及其對空氣品質影響的連續監測，具有明顯提升科學理解力及預測的潛力。

(五) 溫室氣體減排策略效果（包括投資目標）很大程度取決於溫室氣體盤查的準確性。因此，這些盤查必須以最新的科學為依據。澳洲溫室氣體盤查幾乎是使用「自下而上」的方法，已被證明有很大的不確定性，並且可能無法解釋大的潛在來源，因此，2019 年聯合國政府間氣候變化專門委員會(IPCC)排放報告指南也進行修訂，以鼓勵更多地使用「自上而下」的方法，世界氣象組織(WMO)最近也提議擴大全球溫室氣體監測系統。澳洲在溫室氣體量測和通量反演建模已有專業知識，並在全球、區域及局部尺度上，應用自上而下的方法取得了良好的成績，但對國家排放驗證的貢獻受到觀測稀疏性的限制，目前只有 4 個長期站點，但覆蓋的面積卻與歐洲或美國相當，導致對衛星和短期觀測（如實驗計畫）的依賴程度相對較高。

肆、 心得與建議

一、 心得：

(一) 透過本次拜訪加州空氣資源局(CARB)許英光博士及參加美國國家海洋暨大氣總署(NOAA)年會，了解美國及其他國家對於溫室氣體監測的方法，因國外幅員遼闊，不易廣布地面監測站，多數依賴衛星遙測及機載觀測補足空間的不足，但我國因不易發射衛星，故衛星遙測資料的取得可能會受限於資料是否開放或有無完成合作協議。因此，衛星應用雖是未來各項監測之發展趨勢，但仍應先確保資料來源及其代表性與適宜性，以利長期發展運用。

(二) 另衛星並非所有污染源排放皆可觀測到，如美國監測甲烷(CH_4)洩漏，只有大型的污染源排放才可能被偵測到，因此，臺灣是否適用或需要，亦須進行評估。如欲使用相關資料，應先說明其限制，避免各界引用錯誤造成誤解。

(三) 韓國國家環境研究院(NIER)所發射並搭載地球同步環境監測光譜儀(GEMS)，對東亞地區空氣品質監測有很大助益，尤其每年秋冬季節境外污染對臺灣的影響，可以透過相關資料進行模式改善,惟目前本署仍持續透過中央氣象局協助洽詢中，如能取得相關資料，可有效提升本署空品預報能力。

二、 建議事項

(一) 為配合溫室氣體淨零排放長期目標，參考各國對溫室氣體環境監測，並要求資料的掌握程度及有效性，考量我國各項監測發展現況，建議可以地面監測為主，加上國內日益成熟的機載觀測，最後輔以衛星遙測補足空間的不足，建構完整的監測網。

(二) 參加研討會透過各界專家學者的口頭報告及海報論文發表，可在短時間大量蒐集國外發展現況及當前技術，但若對部分

主題或內容欲深入瞭解可能仍屬有限。因此，未來除參與國際上相關研討會，建議若美國國家海洋暨大氣總署(NOAA)或美國國家航空暨太空總署(NASA)等有辦理相關 Workshop（專題討論會、工作坊），可以此優先報名參與，學習包含溫室氣體、空氣污染物等監測儀器操作與技術、衛星資料反演與應用等，成果將可更加豐碩。

附錄 1、投稿海報

Variations of Carbon Cycle Greenhouse Gases in the South China Sea

Chang-Feng Ou-Yang[1], Saginela Ravindra Babu[1], Jense Chiu[1], Edward J. Dlugokencky[2], Don H. Neff[2], Russell C. Schnell[2], Yu-Chen Chiu[3], Jhih-Yuan Yu[3], Chien-Wei Huang[2], Ping-Fei Shieh[3], Neng-Huei Lin[1, 4]

[1]Department of Atmospheric Sciences, National Central University, Taoyuan, Taiwan.
[2]NOAA/GML, Boulder, CO.
[3]Department of Environmental Monitoring and Information Management, Environmental Protection Administration, Taiwan.
[4]Center for Environmental Monitoring and Technology, National Central University, Taoyuan, Taiwan.
Presenter: cfouyang@cc.ncu.edu.tw

Introduction

The South China Sea (SCS) is the largest marginal sea in the world, covering an area from 99°E to 121°E and from the equator to 23°N. It is subject to physical disturbances during various periods of time in a range from short-term events (e.g. typhoons) to seasonal changes (e.g. alternating Asian monsoons) as well as inter-annual oscillations (e.g. El Niño and Southern Oscillation). The prevailing winds in the SCS typically blow from the northeast in winter and from the southwest in summer. During winter, the cold surges driven by frontal passages can carry polluted air masses into the SCS. Furthermore, substantial fire activities associated with agriculture begin in the maritime Southeast Asia in July and end at the onset of the winter monsoon from October to November. These events may increase the concentrations of carbon cycle greenhouse gases in the SCS region.

Fig. 1 Location of Dongsha Island (DSI) and Taiping Island (TPI) in the South China Sea (SCS)

Methods

Flask air samples were collected once per week at two island sites, i.e., Dongsha Island (20.699°N, 116.730°E; code: DSI) and Taiping Island (10.379°N, 114.371°E; code: TPI), located in the northern and southern SCS (Fig. 1), respectively. Both sites are participated in the NOAA/CCGG cooperative air sampling network.

Results and Discussion

This study presents the preliminary results of CO_2, CH_4, and CO observed at DSI and TPI in the SCS from May 2019 to November 2022. As shown in Fig. 2, distinct seasonal variations were found for all the compounds at both sites. However, higher wintertime maxima were observed at DSI than TPI in response to the Asian continental outflow driven by northeast monsoon. In contrast, summertime seasonal minimum levels at DSI and TPI were close to each other. A significant CO peak with a monthly mean of 287.0 ppb was observed at TPI in September 2019, which was suggested being related to the severe biomass-burning episode in Sumatra and Kalimantan, Indonesia, as indicated by VIIRS AOD data (Fig. 3). However, the change was insignificant for CO_2 and CH_4 compared to CO in this case. Furthermore, the biomass-burning plume did not spread to northern SCS, thus no such strong enhancement in CO was observed at DSI.

Similar backward trajectory paths at the two sites as identified by cluster analysis were selected to calculate their differences in concentration (group D3 and T3 as shown in Figs. 4 and 5). For the same origins of air masses associated with Asian continental outflow, the differences in CO_2, CH_4, and CO were 6.0 ppm, 54.1 ppb, and 89.7 ppb, respectively, between DSI and TPI.

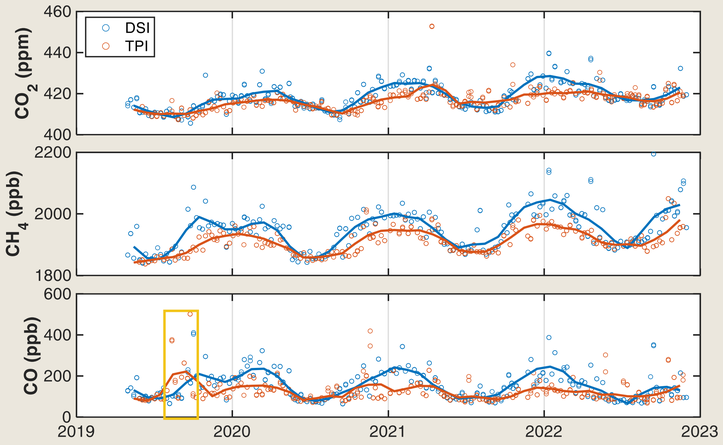

Fig. 2 Temporal variations of CO_2, CH_4, and CO observed at DSI and TPI. The CO peak highlighted in yellow could be associated with the severe biomass burning episodes in September, 2019, as illustrated in Fig. 3.

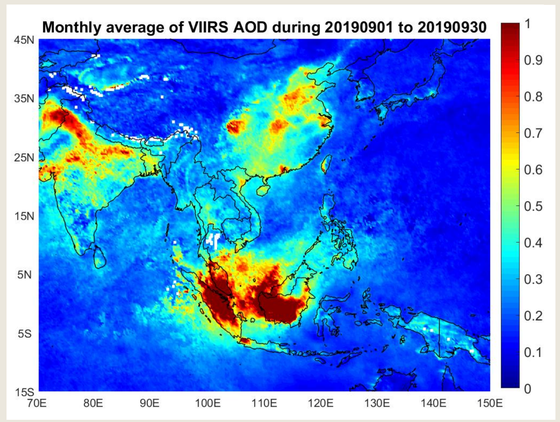

Fig. 3 Monthly average of VIIRS AOD data in East Asia in September, 2019.

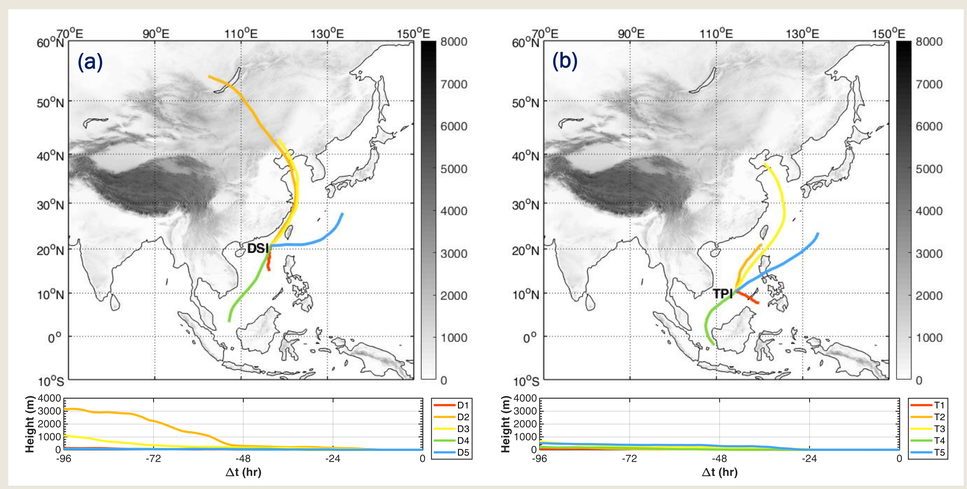

Fig. 4 Cluster analysis of four-day backward trajectories arriving at (a) DSI and (b) TPI.

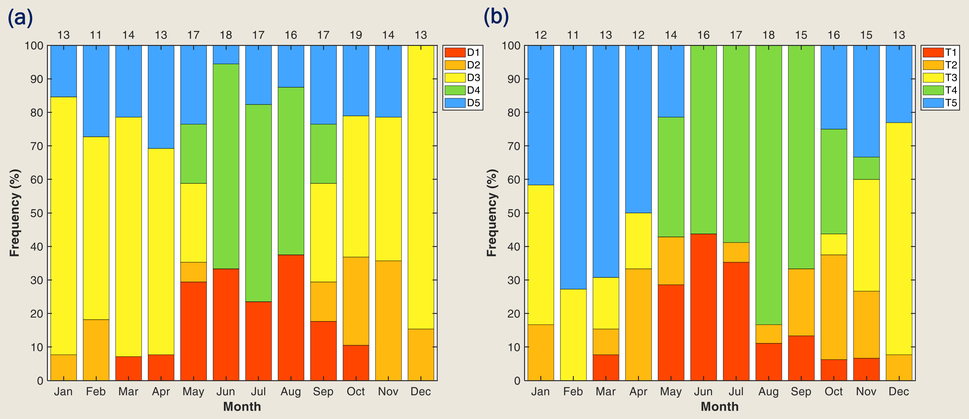

Fig. 5 Frequencies of classified trajectories arriving at (a) DSI and (b) TPI in each month. The number of trajectories calculated is listed on the top.

Origins of Air Masses over the Free Troposphere in Subtropical East Asia: Analysis of Backward Trajectories at Lulin Atmospheric Background Station

Chang-Feng Ou-Yang[1], Chia-Ching Lin[1], Ming-Cheng Yen[1], Yu-Chen Chiu[2], Jhih-Yuan Yu[2], Chien-Wei Huang[2], Ping-Fei Shieh[2], Neng-Huei Lin[1,3]

[1]Department of Atmospheric Sciences, National Central University, Taoyuan, Taiwan.
[2]Department of Environmental Monitoring and Information Management, Environmental Protection Administration, Taiwan.
[3]Center for Environmental Monitoring and Technology, National Central University, Taoyuan, Taiwan.
Presenter: cfouyang@cc.ncu.edu.tw

Introduction

The Lulin Atmospheric Background Station (23.47°N, 120.87°E, 2862 m a.s.l.; code: LLN) lies in the free troposphere of subtropical East Asia and has been operated since April 2006. As shown in Fig 1, LLN is a two-story building located at the mountaintop of Mt. Front Lulin in Yushan National Park in central Taiwan with no known strong emissions in the proximity of the station. The local vegetations are mainly hemlocks and spruces within the altitude range of 2500-3100 m. Various observation programs have been conducted at LLN, including meteorology, acid precipitation, trace gases, atmospheric mercury, aerosol physical and chemical properties, and solar radiations.

Methods

Five-day (120 h) backward trajectories arriving at LLN were simulated using NOAA/ARL HYSPLIT version 4 model. The meteorological grid data used were the Global Data Assimilation System (GDAS1 archive) provided by the National Center for Environmental Prediction (NCEP) with a 6 h time resolution, a 1°×1° latitude-longitude (360 by 181) resolution, and 24 vertical levels. All back-trajectories were computed at a frequency of 1 synoptic time per day during the intensive biomass burning period from mid-February to mid-April each year.

Fig. 1 The Lulin Atmospheric Background Station (code: LLN)

Results and Discussion

Based on the HYSPLIT backward trajectory analysis using NCEP/GDAS1 meteorological dataset, oceanic influences from the Pacific were predominant in summer, leading to seasonal minima for most species. In contrast, the springtime air masses mainly originated from northern mainland Southeast Asia in association with biomass burning emissions, causing seasonal maxima of most air pollutants. However, the springtime footprints changed significantly during 2015-2018 (Fig. 2), likely due to the magnified vertical velocity provided in GDAS1 from 2015 to mid-2017 (Fig. 3). Such hiatus was absent if GDAS0.5 was used. The GDAS0.5 dataset does not provide vertical velocity; thus, the HYSPLIT model calculates vertical velocity from divergence. In addition, no significant changes in the wind patterns observed at LLN were found during the same period (Fig. 4).

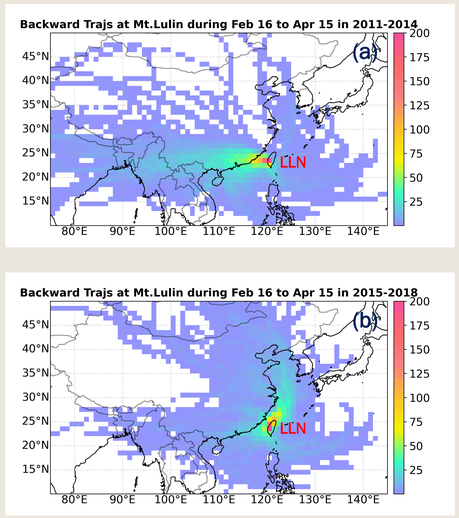

Fig. 2 Backward trajectories arriving at LLN in spring during (a) 2011-2014 and (b) 2015-2018.

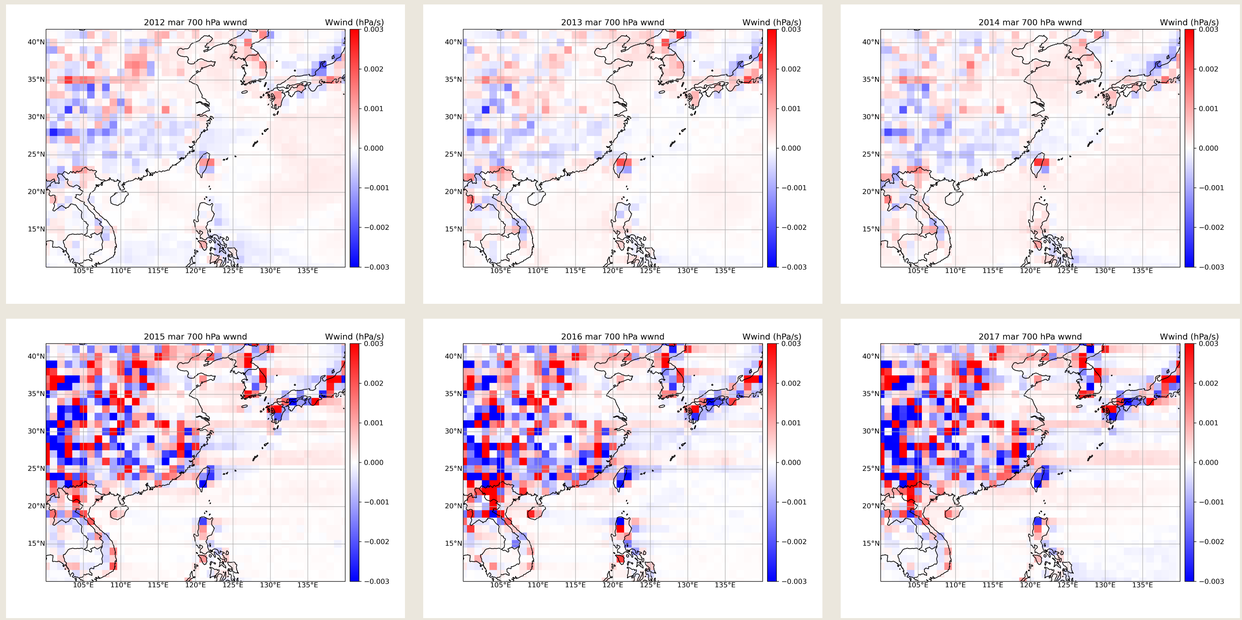

Fig. 3 Pressure vertical velocity for the East Asia from GDAS1 dataset in March from 2012 to 2017.

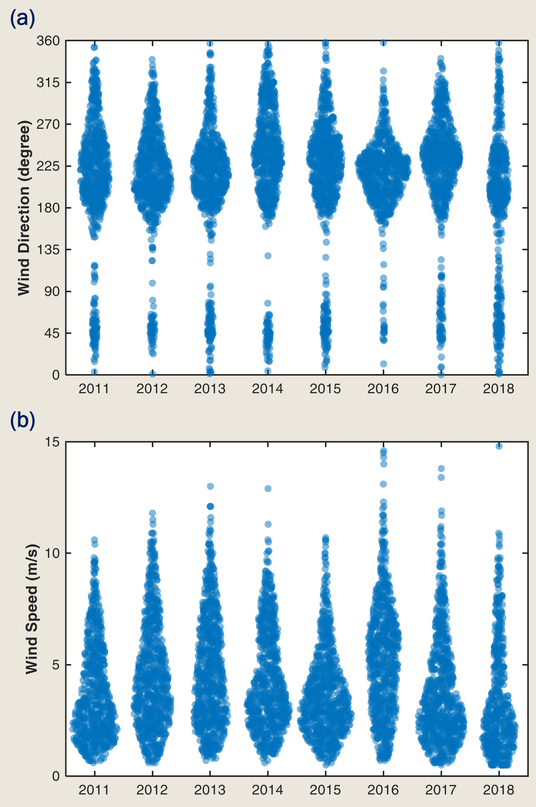

Fig. 4 (a) Wind direction and (b) wind speed observed at LLN in March from 2011 to 2018.

附錄 2、出國期間照片

圖 1.與國立中央大學歐陽長風博士（圖右）拜會加州空氣資源局(CARB)許英光博士（圖中）

圖 2. 與 NOAA 全球監測實驗室(GML)主任 Vanda Grubišić 博士（左二）及國立中央大學歐陽長風博士（右二）黃翔昱博士（右一）攝於會場

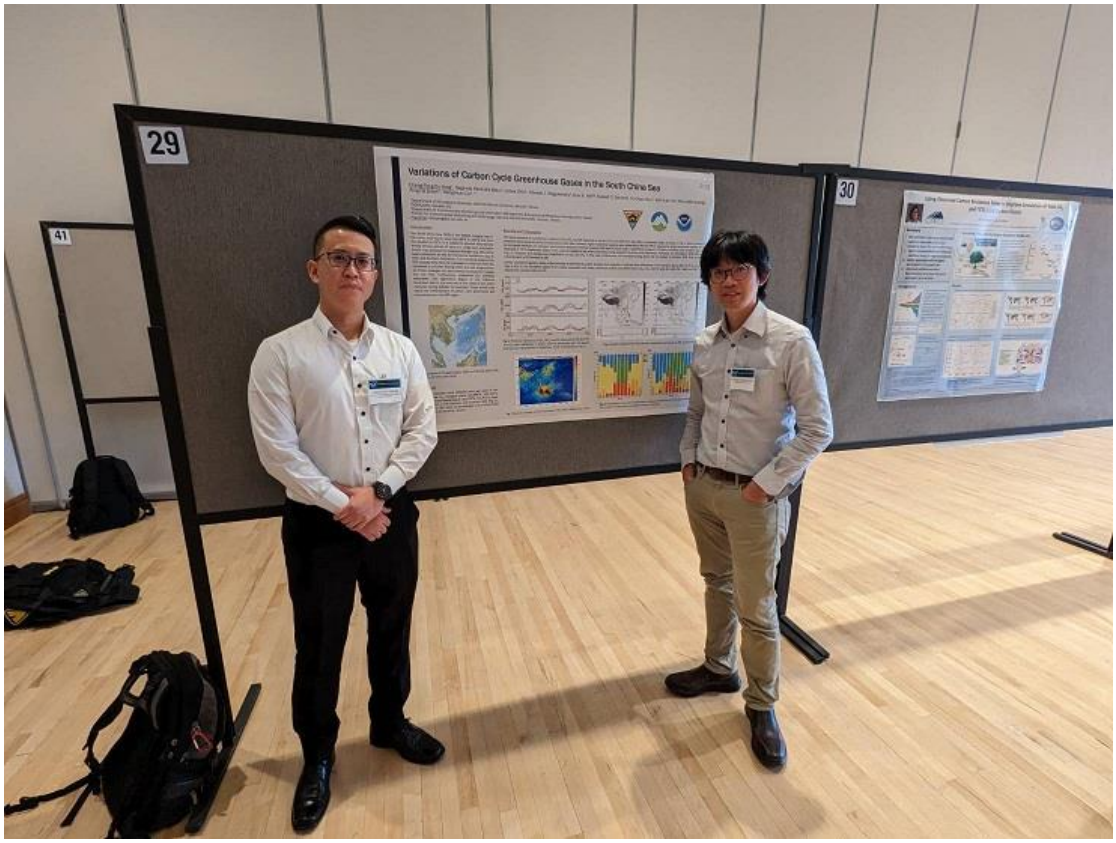

圖 3．與國立中央大學歐陽長風博士（圖右）攝於海報展示會場

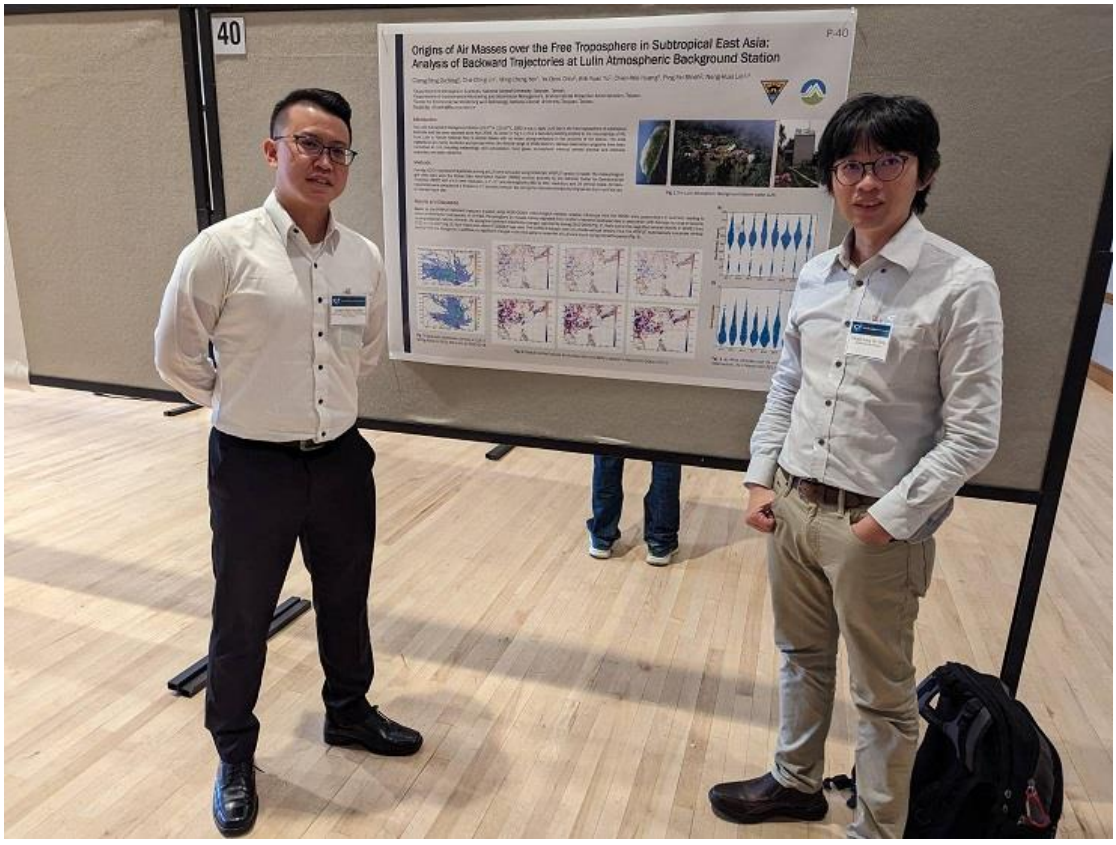

圖 4．與國立中央大學歐陽長風博士（圖右）攝於海報展示會場

圖 5.國立中央大學黃翔昱博士報告鹿林山大氣背景站監測成果

附錄 3、會議資料

Keynote Address: **The 2022 Hunga Tonga-Hunga Ha'apai Eruption: NOAA's Rapid Response**

K. Rosenlof

NOAA Chemical Sciences Laboratory (CSL), Boulder, CO 80305; 303-578-0651, E-mail: karen.rosenlof@noaa.gov

The Hunga Tonga - Hunga Ha'apai (HTHH) volcano, located in South Pacific, erupted on Jan. 13 and 15, 2022, putting significant amounts of material into the stratosphere. The lower stratospheric winds at the time of the eruption were blowing toward the west, with expected transit of the volcanic plume to over Reunion Island in about a week. As there had not previously been fresh in situ stratospheric measurements of a volcanic plume that soon after eruption, efforts were made to bring aerosol and SO_2 in situ balloon payloads to Reunion Island immediately after the eruption. This was only possible because of the existing Balloon Baseline Stratospheric Aerosol Profiles (B^2SAP) program. Measurements of the HTHH plume showed extremely large water vapor perturbations due to the eruption, and further analysis has shown that the water vapor excess accelerated conversion of SO_2 gas to sulfate aerosol. Modeling work is ongoing to understand possible impacts on stratospheric ozone and dynamics over the next few years.

The Evolution of SF_6 as an Age of Air Tracer

E. Ray[1], F.L. Moore[2,3], E. Hintsa[2], B.D. Hall[3], G. Dutton[2,3], D. Nance[2,3], H. Garny[4], B. Baier[3], J. Li[2,3], and C. Sweeney[3]

[1]NOAA Chemical Sciences Laboratory (CSL), Boulder, CO 80305; 303-579-2958, E-mail: eric.ray@noaa.gov
[2]Cooperative Institute for Research in Environmental Sciences (CIRES), University of Colorado, Boulder, CO 80309
[3]NOAA Global Monitoring Laboratory (GML), Boulder, CO 80305
[4]German Aerospace Center (DLR), Institute of Atmospheric Physics, Oberpfaffenhofen-Wessling, Germany

The long lifetime and steady growth rate of sulfur hexafluoride (SF_6) have made it a useful trace gas to estimate the age of air in the atmosphere. This estimation is complicated somewhat by the loss of SF_6 in the lower mesosphere due to free electron association. Mesospheric air with SF_6 loss is transported down into the stratosphere, especially in the winter polar vortices where mean age derived from SF_6 has been shown to be biased old due to the presence of air with substantial SF_6 loss. Recent theoretical and modeling work has shown that since the amount of SF_6 loss is proportional to the mixing ratio, which has grown larger by several times over the past few decades, the deviation of SF_6 mean ages from the ideal mean age is also expected to have grown larger over this time period. In this work we compare mean age estimates from aircraft campaign and balloon measurements of SF_6, as well as other mean age tracers such as CO_2 and nitrous oxide (N_2O), over the past several decades, including measurements from the recent DCOTTS and SABRE aircraft missions and AirCore flights. We use a newly developed correction technique to adjust observed SF_6 mean ages based on the year and latitude of the measurements to help evaluate the theoretical and model-based estimates of the evolution of SF_6 mean age biases over time.

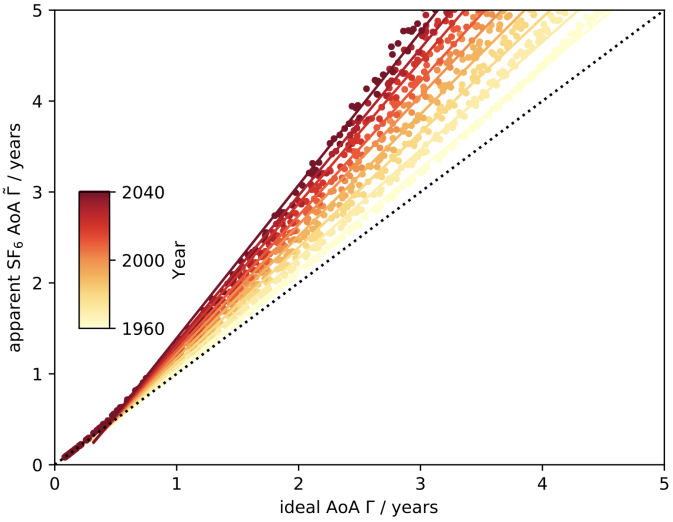

Figure 1. Theoretical SF_6 mean age bias compared to idealized modeled mean ages colored by year from 1960-2040.

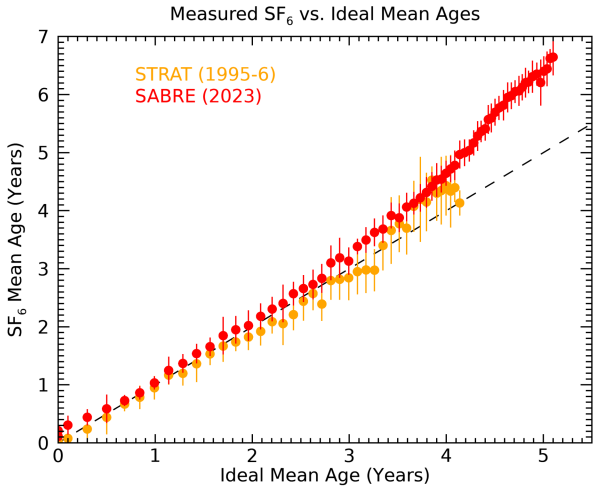

Figure 2. SF_6 mean ages from the STRAT (1995-6) and SABRE (2023) aircraft campaigns vs. an idealized mean age based on CO_2 and N_2O measurements from many aircraft campaign measurements.

Emissions of CF_4 (PFC-14) and C_2F_6 (PFC-116) in China Inferred from a Chinese Atmospheric Observation Network

M. An[1,2], R. Prinn[1], L.M. Western[2,3], B. Yao[4,5], J. Hu[6], and M. Rigby[2]

[1]Massachusetts Institute of Technology, Center for Global Change Science, Cambridge, MA 02139; 617-583-0020, E-mail: mindean@mit.edu
[2]University of Bristol, School of Chemistry, Bristol, United Kingdom
[3]NOAA Global Monitoring Laboratory (GML), Boulder, CO 80305
[4]Fudan University, Department of Atmospheric and Oceanic Sciences & Institute of Atmospheric Sciences, Shanghai, China
[5]Meteorological Observation Centre of China Meteorological Administration (MOC/CMA), Beijing, China
[6]Peking University, College of Environmental Sciences and Engineering, Beijing, China

The perfluorocarbons (PFCs) are potent non-CO_2 Greenhouse Gases controlled by the Paris Agreement under the United Nations Framework Convention on Climate Change (UNFCCC). The PFCs tetrofluoromethane (CF_4, PFC-14) and hexafluoroethane (C_2F_6, PFC-116) are the two most abundant PFCs in the atmosphere, with global warming potentials of 7,380 and 12,400 respectively over a 100-year time horizon (GWP_{100}), and atmospheric lifetimes of 50,000 and 10,000 years, respectively.

An atmospheric observation network consisting of nine sites located across China has made atmospheric measurements of CF_4 and C_2F_6 since 2012 and 2011 respectively. These observations provide good sensitivity to emissions in most of the important regions of China (Figure 1). Emissions of the two substances in China over the last decade (2011-2020) were derived from the observations and a top-down Bayesian inverse modelling approach. Emissions of both substances in China show a substantial increase since measurements in China began. Emissions inferred by measurements in China are larger than emissions inferred from atmospheric observations made outside China (e.g., Kim et al., 2021). The difference is likely due to substantial emissions from the western regions of China to which observations outside China (e.g., made at Gosan in South Korea) do not have sufficient sensitivity. Significant leakages of CF_4 and C_2F_6 can occur during the large volume of aluminum and magnesium production in the western regions.

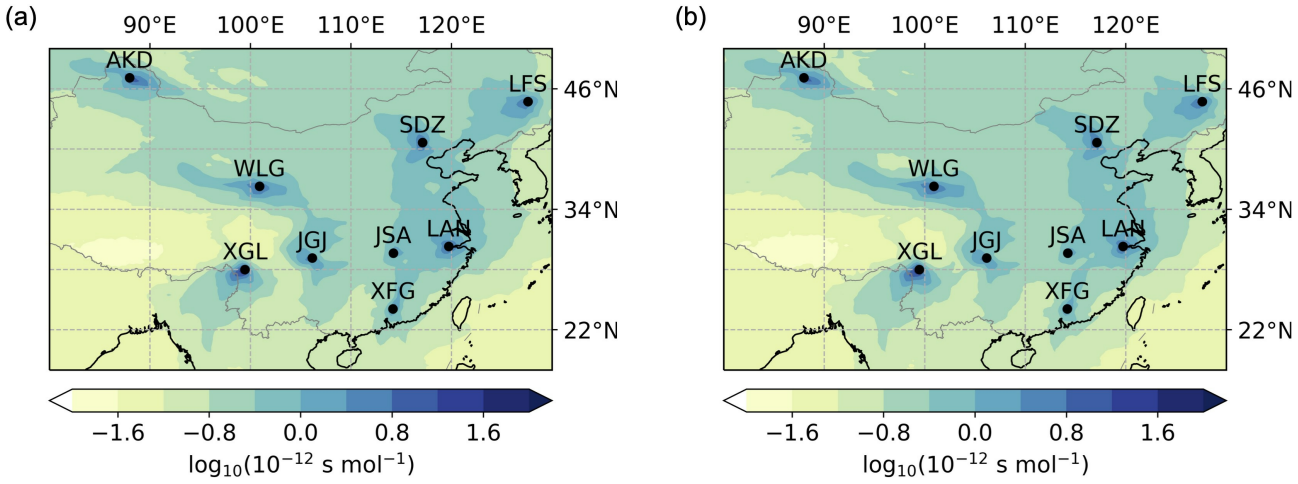

Figure 1. Locations of the measurement sites in the Chinese network. The color in the plot represents the sensitivity of all the observations to emissions in China, an average of the sensitivity in each year from all sites. Plot (a) is for CF_4 over 2012-2020 and (b) is for C_2F_6 over 2011-2020.

Halocarbons Observations in the Himalaya

M. Maione[1,2], J. Arduini[1], P. Bonasoni[2], Z. Cong, Y. Chen, E. Saikawa[3], T. Yao, Q. Zhang, M. Xie, L. Tan, and X. Wan

[1]University of Urbino, Department of Basic Sciences and Foundations, Urbino, Italy; +393404157897, E-mail: michela.maione@uniurb.it
[2]Institute of Atmospheric Sciences and Climate, National Research Council of Italy, Bologna, Italy
[3]Emory University, Department of Environmental Sciences, Atlanta, GA 30322

The Himalayas and the Tibetan Plateau (HTP) is a vast geographic area, covering ~ 5 million km^2 and an average altitude of more than 4000 m (a.s.l) located between South and East Asia, two emission hot spots for several anthropogenic species, including the ozone-depleting (ODSs) and radiatively active halocarbons. Despite its crucial location, HTP is an under-sampled region with sparse measurements. Here we report the results from two field campaigns carried out in April and May 2022 at the Nepal Climate Laboratory-Pyramid station (27.95°N, 86.82°E, 5079 m a.s.l., NCO-P) in the high Khumbu valley, on the southern side of the Mt. Everest and at Mt. Everest (Qomolangma) base camp (28.19°N, 86.83°E, 5010 m a.s.l), respectively. During the campaigns, flask samples were collected, and 36 halocarbons were measured through Gas Chromatography-Mass Spectrometry. A comparison between the results from the 2022 campaigns and data from a monitoring programme running during 2008-2013 at NCO-P are also presented. The dominant ODSs exhibited a declining trend, reflecting the effectiveness of the Montreal Protocol. On the other hand, a large increase in HFCs and a high abundance of unregulated chlorocarbons (e.g., CH_3Cl) is shown.

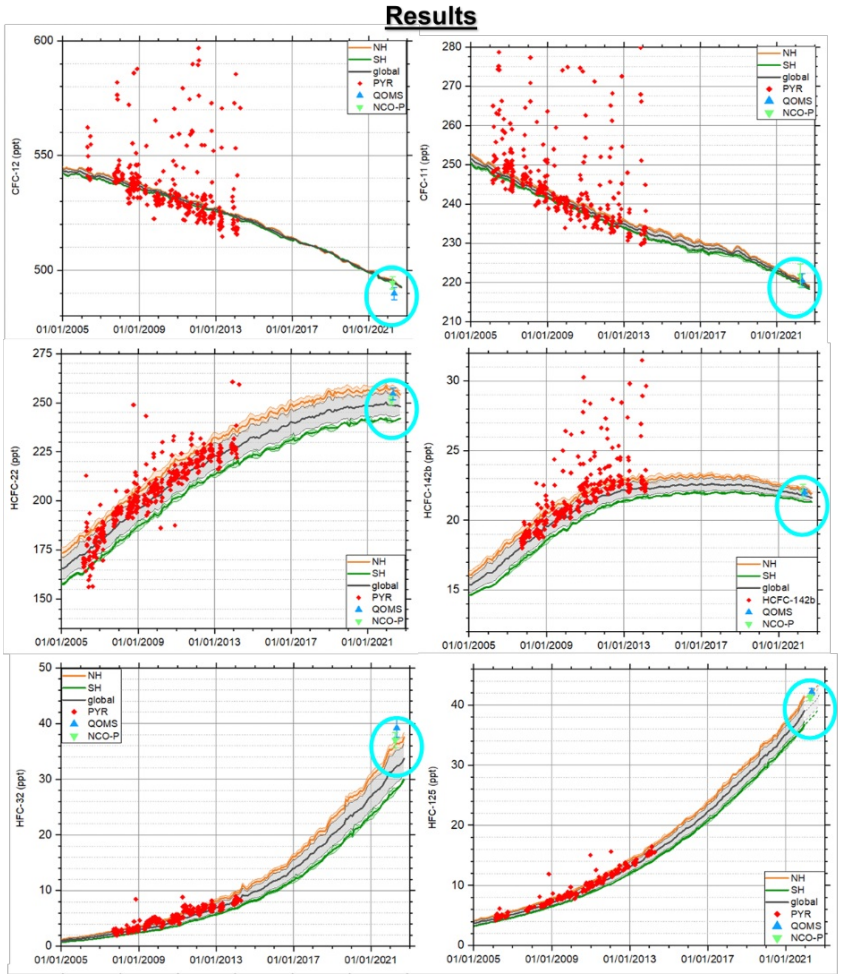

Figure 1. Halocarbons in the Himalayas and comparison with global, Northern Hemisphere and Southern Hemisphere average values

Halogen-containing Compounds in the Lower Stratosphere during the North American Summer Monsoon Season

E. Hintsa[1], F.L. Moore[1,2], G. Dutton[1,2], J.D. Nance[1,2], J.W. Elkins[3], B. Hall[2], K. Smith[4], S. Donnelly[4], S. Schauffler[5], V. Treadaway[4], E. Atlas[4], P. Bui[6], D. Wilmouth[7], and J. Smith[7]

[1]Cooperative Institute for Research in Environmental Sciences (CIRES), University of Colorado, Boulder, CO 80309; (720) 514-9637, E-mail: Eric.j.hintsa@noaa.gov
[2]NOAA Global Monitoring Laboratory (GML), Boulder, CO 80305
[3]Retired from NOAA Global Monitoring Laboratory (GML), Boulder, CO 80305
[4]University of Miami, Rosenstiel School of Marine and Atmospheric Sciences, Miami, FL 33173
[5]National Center for Atmospheric Research (NCAR), Boulder, CO 80307
[6]NASA Ames Research Center, Moffett Field, CA 94035
[7]Harvard University, Cambridge, MA 02138

Intense convection occurs in summer within the North American Monsoon Anticyclone (NAMA) circulation, with over 100 storms penetrating the tropopause daily. These storms can inject water vapor and other chemicals into the lower stratosphere, with unknown effects on stratospheric ozone. The Dynamics and Chemistry of the Summer Stratosphere (DCOTSS) mission was designed to study this coupled dynamical and chemical system, and included deployments of the ER-2 aircraft from Salina, KS, along with radar, satellite and sonde observations of atmospheric structure and convection. We present measurements and analysis of organic and inorganic halogen-containing compounds from DCOTSS 2021. Long-lived anthropogenic halocarbons, such as CFCs and halons, are broken down at high altitudes before descending into the lower stratosphere. Shorter-lived compounds have both anthropogenic and natural sources, and can enter the stratosphere from the tropics or via direct injection by convection at mid-latitudes. Photochemical destruction of these compounds releases inorganic chlorine and bromine, which can lead to halogen-catalyzed ozone loss. The UAS Chromatograph for Atmospheric Trace Species (UCATS) measures several long- and short-lived organic chlorine species, accounting for about 2/3 of organic chlorine, and the Advanced Whole Air Sampler (AWAS) measures a comprehensive suite of trace gases, including most organic chlorinated and brominated halocarbons of interest, allowing an analysis of the organic chlorine budget of the lower stratosphere at the higher time resolution of the UCATS instrument, using AWAS samples to account for unmeasured species. We also calculate the approximate total amount of chlorine entering the stratosphere from the NOAA surface network and UCATS measurements of SF6, a tracer of mean age of air. From the difference between total chlorine and remaining organic chlorine, we estimate the amount of inorganic chlorine in each sample. We show results on total organic chlorine over North America in summer 2021, in background stratospheric air as well as in convectively influenced air and plumes of recent convection, with estimates of the amount of available inorganic chlorine and measurements of some of the important inorganic chlorine species.

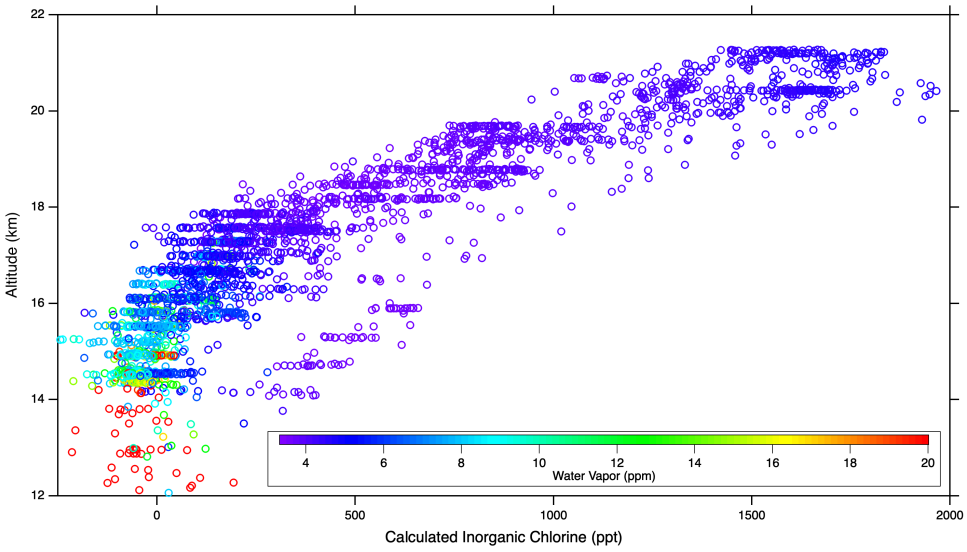

Figure 1. Calculated inorganic chlorine (Cly) in the stratosphere over the North American Monsoon circulation, color-coded by water vapor. Enhanced water vapor, which could activate chlorine, was only present in air parcels with low Cly measured in 2021.

Investigating Trace Gases other Than CH3CCl3 for Supplying Useful Information About Atmospheric Hydroxyl Radical Abundance and Variability on Broad Scales.

S. Montzka[1], I. Vimont[2,1], F.L. Moore[2,1], G.S. Dutton[2,1], B. Hall[1], S. Clingan[2], and K. Petersen[2]

[1]NOAA Global Monitoring Laboratory (GML), Boulder, CO 80305; 720-295-9701, E-mail: stephen.a.montzka@noaa.gov
[2]Cooperative Institute for Research in Environmental Sciences (CIRES), University of Colorado, Boulder, CO 80309

Constraints on hemispheric- to global-scale hydroxyl radical concentrations [OH] are important for understanding changes in the atmospheric abundance of methane and other long-lived gases primarily removed from the atmosphere via oxidation by OH. The usefulness of constraints on [OH] supplied by the analysis of CH_3CCl_3 observations has degraded in recent years, such that alternative approaches are desperately needed. We have investigated other trace gases for supplying constraints on [OH] using approaches that are less sensitive to budget considerations, given that independent estimates of emissions required for such approaches often contain substantial uncertainties that are difficult to assess. Many gases we regularly measure exhibit atmospheric distributions that clearly reflect loss due to OH oxidation processes. Initial results suggest that an analysis of these distributions can provide insights into OH concentrations on broad atmospheric scales. In this presentation we'll investigate the robustness of those constraints and their sensitivity to parameters such as mean transport times for air between the hemispheres, among other processes and variables.

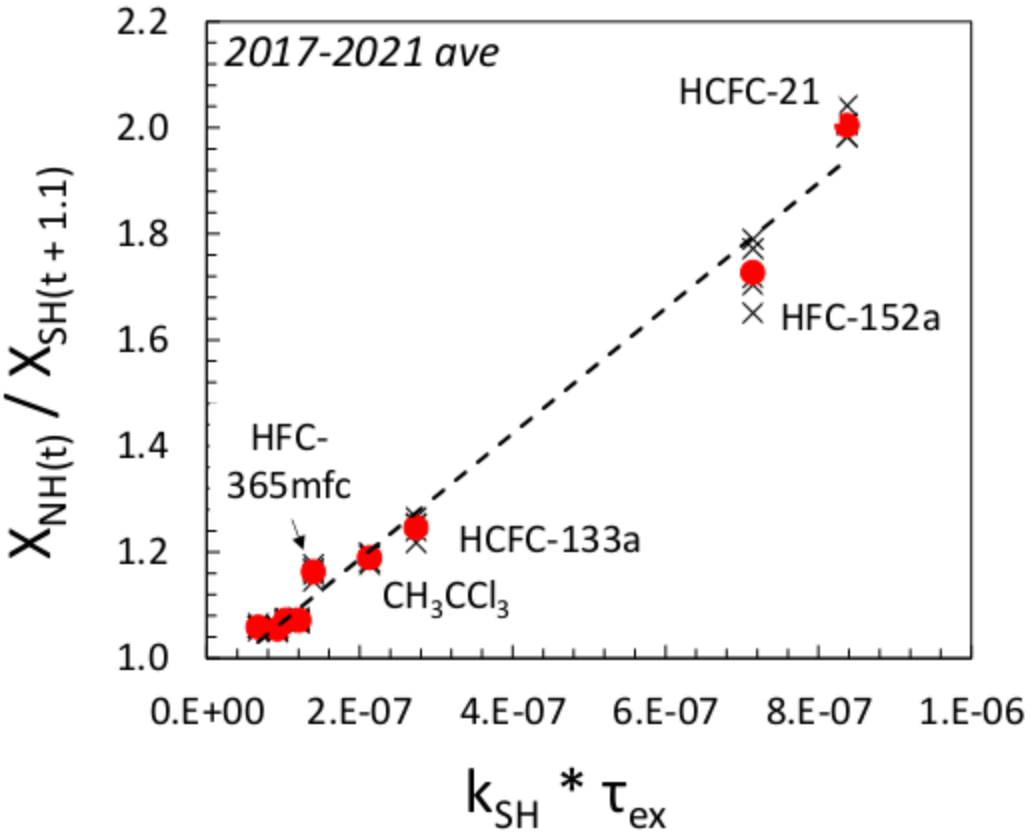

Figure 1. The lagged mean hemispheric mole fraction difference observed for multiple trace gases from 2017-2021 as a function of their rate constant for reaction with the hydroxyl [OH] radical. The slope in this plot (1.2 x 10^6 radicals cm^3) is thought to provide an estimate mean of OH concentration for the tropics and much of the southern hemisphere.

Monitoring Lower Stratospheric Composition from Space using Reanalysis of NASA Satellite Observations in the EOS and Post-EOS Era

S. Pawson[1], K.E. Knowland[2], P. Wales[2], K. Wargan[1], and B. Weir[3,1]

[1]NASA Goddard Space Flight Center (GSFC), Greenbelt, MD 20771; 240-397-1481, E-mail: Steven.Pawson-1@nasa.gov
[2]NASA Goddard Space Flight Center (GSFC), Global Monitoring and Assimilation Office, Greenbelt, MD 20771
[3]Universities Space Research Association (USRA), Colombia, MD 21046

NASA's Modern-Era Retrospective analysis for Research and Applications (MERRA-2) reanalysis assimilates observations from a wide variety of sources, including the Earth Observing System (EOS) platforms. Stratospheric ozone profile data from the Microwave Limb Sounder (MLS) on EOS Aura represent a consistent ozone time series since 2004, that captures the large signal of interannual transport variations which dominate the recovery trend in the lower stratosphere since the early 2000s. In addition, the MERRA-2 Stratospheric Composition Reanalysis of Aura MLS (M2-SCREAM) further presents a more complete data series of assimilated stratospheric constituents, allowing for the investigation of long-term changes in water vapor and other key gases, in context of the dynamic atmosphere.

With the planned decommissioning of the EOS platforms within the next two years, the continuity of the climate records for atmospheric constituents will be broken. This presentation gives an overview of how feasible it is to maintain a comprehensive record of ozone and water vapor in the stratosphere using alternative instruments currently still in orbit. For ozone, the OMPS-LP observation record from the Suomi-NPP and the JPSS-2 platforms provide suitable spatio-temporal coverage to extend the utility of multi-platform reanalyses in the lower to middle stratosphere. For water vapor, information from the SAGE-III occultation instrument aboard the International Space Station provides information that has potential for maintaining the record in a limited latitude band. The discussion includes some examples of steady changes and of extreme events that occurred over the almost two decades of MLS observations.

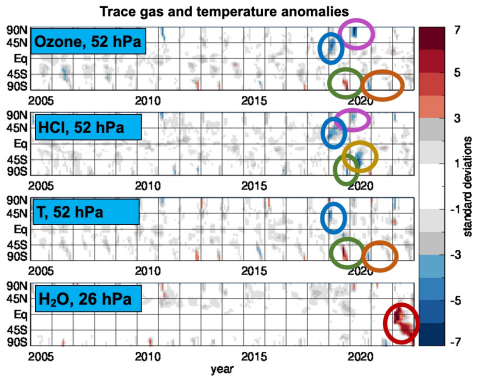

Figure 1. Stratospheric extrema from a chemical reanalysis of Aura MLS observations. Monthly mean detrended anomalies of ozone, (HCl), temperature, and water vapor at selected pressure levels, calculated from M2-SCREAM. Values outside three-standard deviations from the mean are shown in color. Here, the standard deviations are computed over the 17-year period between 2005 and 2021. The colors illustrate: a dynamically driven anomaly in early 2019 (blue); a rare sudden stratospheric warming over Antarctica in late 2019 (green); an exceptionally string Arctic polar vortex in 2020 (purple); long-lasting Antarctic polar vortices in 2020 and 2021 (orange); and the Hunga-Tonga Hunga-Ha'apai (HTHH) eruption in 2022.

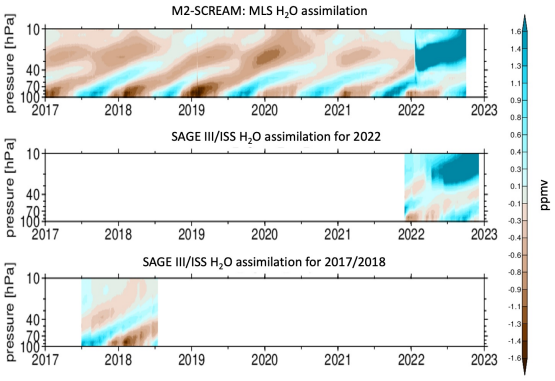

Figure 2. Illustrating the potential continuity of stratospheric moisture in reanalyses as we transition from MLS to SAGE III/ISS observations.

Time series of tropical stratospheric water vapor anomalies from M2-SCREAM (MLSassimilation) and two SAGEIII/ISS assimilation experiments. Good representation of the seasonal pattern ("tape recorder") and the moisture enhancement from the Hunga-Tonga Hunga-Ha'apai (HTHH) eruption in 2022 demonstrates usefulness of SAGE III/ISS data for reanalyses. MLS data post 2023 will be essential for homogenization as the impacts of HTHH on the stratosphere continue.

CarbonTracker Long-window for Multi-tracer Data Assimilation

J. Hooghiem[1], J.B. Miller[2], A. Kaushik[3,2], S. Michel[4], D. Munro[3,2], X. Lan[3,2], A.E. Andrews[2], A. van der Woude[1], A. van den Berg[1], L. Florentie[1], G. Koren[1], R.D. Kok[1], I. van der Laan-Luijkx[1], and W. Peters[1]

[1]Wageningen University, Department of Meteorology and Air Quality, Wageningen, The Netherlands; +316 27476622, E-mail: joram.hooghiem@wur.nl
[2]NOAA Global Monitoring Laboratory (GML), Boulder, CO 80305
[3]Cooperative Institute for Research in Environmental Sciences (CIRES), University of Colorado, Boulder, CO 80309
[4]Institute of Arctic and Alpine Research (INSTAAR), University of Colorado, Boulder, CO 80309

Joint assimilation of atmospheric carbon dioxide mole fractions along with isotopic ratios of $^{13}C/^{12}C$ (denoted $\delta(^{13}C)$) allows for estimation not just of global and regional fluxes of CO_2 but also information on the sensitivity to drought of terrestrial ecosystem CO_2 uptake. In particular, atmospheric $\delta(^{13}C)$ observations allow us to optimize the preference plants have for taking up $^{12}CO_2$ during photosynthesis, i.e., “fractionation”, which is a sensitive indicator of water stress (Fig. 1). Our data assimilation system is a new variant of the CarbonTracker family, but constructed to efficiently process multi-decadal CO_2 and $\delta(^{13}C)$ records and the carbon cycle constraints they provide. Although our new approach is still based on ensembles, TM5 transport modeling is now performed only once for the full multi-decadal time-span and the flux and fractionation optimizations are completed after transport. This contrasts with the existing global CarbonTracker systems (CT-Europe and CT- CO_2) that use a repetitive weekly time-stepping approach where optimization is not separated, and where transport is simulated 6 times. Examples of low frequency processes in the carbon cycle that we target are the isotopic disequilibrium fluxes of the oceans and land. Separating the transport and data assimilation steps is also cheaper numerically, and allows quick tests for the influence of the prescribed model-data mismatch, ensemble size, and site selection. We compare the performance of this new system to an ensemble of other global inversion systems, and benchmark it with independent aircraft data for both CO_2 as well as $\delta(^{13}C)$. The added value of $\delta(^{13}C)$ that we aim to leverage will be shown in a co-optimization of NEE, fractionation, and disequilibrium fluxes.

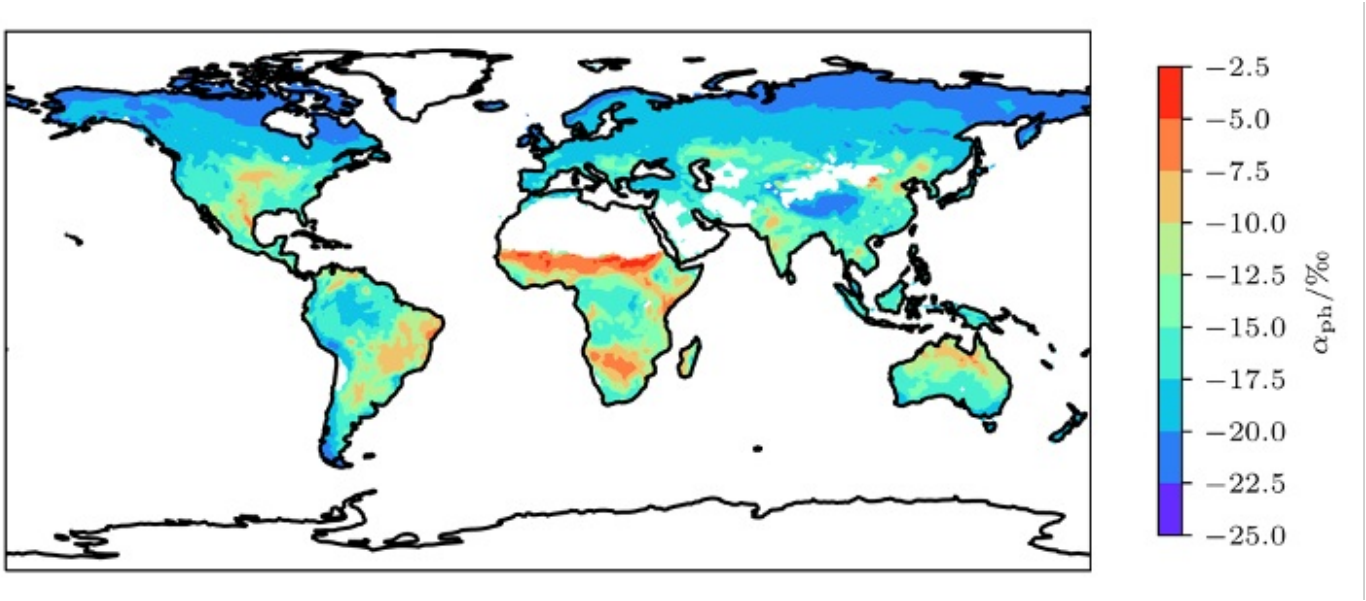

Figure 1. Optimized annual mean photosynthetic fractionation

CarbonTracker-CH_4 2023: An Isotope-constrained Global Methane Inversion

L. Bruhwiler[1], Y. Oh[2,1], and X. Lan[2,1]

[1]NOAA Global Monitoring Laboratory (GML), Boulder, CO 80305; 720-217-6326, E-mail: lori.bruhwiler@noaa.gov
[2]Cooperative Institute for Research in Environmental Sciences (CIRES), University of Colorado, Boulder, CO 80309

Observations indicate accelerating growth of atmospheric CH_4, creating a challenge for meeting the Global Methane Pledge that aims to achieve 30% cuts in emissions by 2030 and eliminate 0.2°C of warming by 2050. In addition, a recent United Nations Environment Programme (UNEP) report proposes that feasible CH_4 emission cuts could result in a 45% reduction in anthropogenic emissions, and avoid 0.3ºC of warming by mid-century while having a positive impact on human health through air quality improvements. However, our understanding of the processes driving CH_4 growth in the atmosphere is incomplete, and we need to understand and be able to discriminate among contributions from chemical, natural and anthropogenic emissions and sinks. In particular, we need to be able to understand how global microbial emissions from both natural and anthropogenic sources are changing over time.

Measurements of the ^{13}C stable isotope of CH_4 could be useful for partitioning emissions between fossil fuel and microbial sources, and these measurements imply that recent increases in atmospheric growth are dominated by microbial sources, likely from a combination of anthropogenic and natural sources. Our new version of the CarbonTracker-CH_4 inverse modeling system uses the isotopic record as a constraint, and as a result global fossil fuel emissions are adjusted upwards while global microbial emissions are adjusted downwards. Our results also show how increases in microbial emissions, especially from the tropics and high northern latitudes have contributed the observed growth in atmospheric CH_4. In this presentation we will highlight findings from CarbonTracker-CH_4 over 1998-2021, and we will discuss major uncertainties and future work.

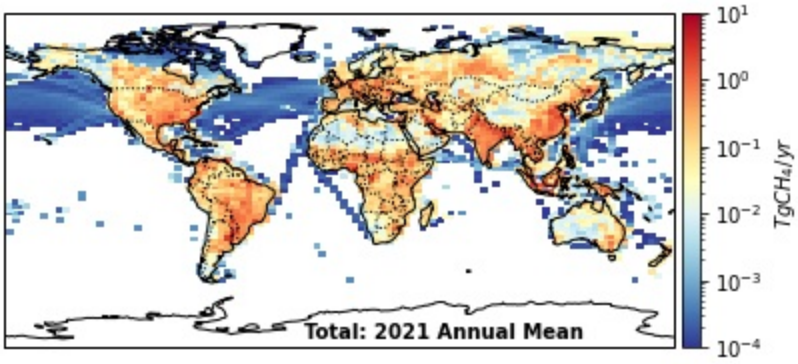

Figure 1. Annual mean emissions for 2021 estimated by CarbonTracker-CH_4

Development of the ECCC's National Scale Carbon Flux Inversion Modelling System

J. Kim[1], M. Neish[1], E. Chan[2], D. Chan[1], M. Ishizawa[2], S. Polavarapu[1], S. Curasi[2], A.E. Andrews[3], L. Hu[3], and D. Worthy[1]

[1]Environment and Climate Change Canada (ECCC), Toronto, Ontario, Canada; 416-739-4928, E-mail: jinwoong.kim@ec.gc.ca
[2]Climate Research Division, Environment and Climate Change Canada (ECCC)
[3]NOAA Global Monitoring Laboratory (GML), Boulder, CO 80305

Canada is the second largest country in the world, with various ecosystems in the Arctic and boreal forest zones. In the coming years, Canada may experience a changing balance between warming, CO_2 fertilization, drought, and shifting disturbance regimes in boreal forests, as well as the changes in greenhouse gas (GHG) emissions as permafrost thaws in response to climate change. Thus, the Environment and Climate Change Canada (ECCC) National Carbon flux Inversion System (ENCIS) was proposed to provide quantitative information on GHG fluxes over Canada from national to provincial scales using atmospheric GHG measurements (e.g., Fig. 1a), as well as to address scientific questions with respect to the carbon cycle in Canada. Although the goal is to quantify the sources and sinks of GHG within provinces and on a national scale, this is a challenging task due to model transport errors and observation sparsity on regional scales. Here, we present the ENCIS development and its application to regional CO_2 inversions for Canada. The ENCIS is a regional-scale inversion modelling system which uses a Bayesian inversion approach described by NOAA's CarbonTracker-Lagrange. The system utilizes multiple transport models, prior fluxes, and background CO_2 components to estimate the uncertainties in the optimized biospheric fluxes. The performance of the inversion system is assessed by performing a set of observing system simulation experiments. In addition, we will also present our flux estimates over Canada using real observations (Fig. 1b).

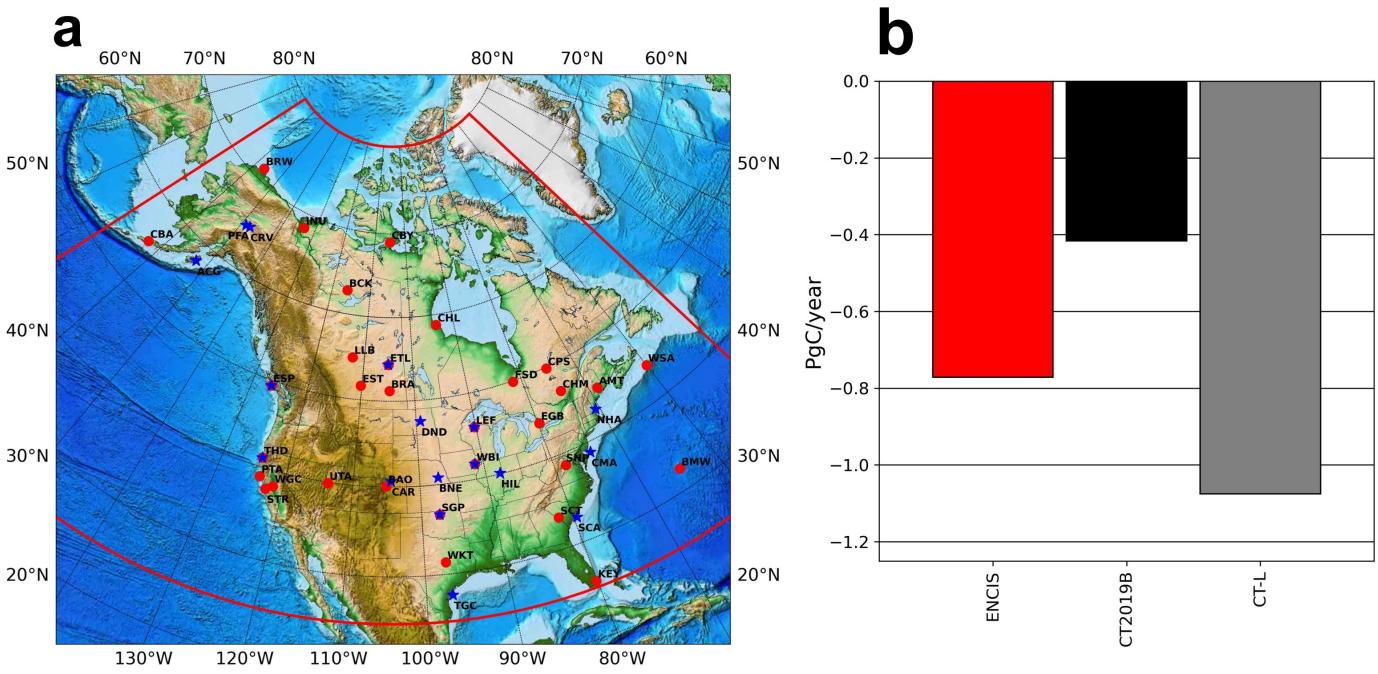

Figure 1. a) The inversion domain of the ENCIS (red solid line) and the observation network used in the experiment (red dot: surface site, blue star: aircraft profile sites). b) A first look at the annual biospheric CO_2 flux estimate over Canada for 2014 (PgC yr^{-1}) from an ensemble of experiments with real observations (red), NOAA's CT2019B (black), and CarbonTracker-Lagrange (grey).

A Zonally Averaged Global Transport model for Long-lived Trace Gases

L. Western[1,2], S. Bachman[3], M. Rigby[1], and S.A. Montzka[2]

[1]University of Bristol, School of Chemistry, Bristol, United Kingdom; 720-319-8482, E-mail: luke.western@bristol.ac.uk
[2]NOAA Global Monitoring Laboratory (GML), Boulder, CO 80305
[3]National Center for Atmospheric Research (NCAR), Boulder, CO 80307

Quantifying global emissions of non-CO_2 greenhouse gases and ozone depleting substances using atmospheric measurements of their abundance is important to understand the environmental impacts of these gases and to monitor compliance with international protocols. The large number of gases of interest – for example clorofluorocarbons (CFC), hydrofluorocarbons (HFC), perfluorocarbons (PFC) – requires atmospheric modelling that is faster and more simplified compared to that of the three major greenhouse gases. Currently, emissions are mainly quantified using simplified box models of atmospheric transport, which neglect the interannual variability in atmospheric large-scale dynamics that is known to impact emissions estimates. Here we propose a two-dimensional model of atmospheric transport, which considers transport variability on a monthly timescale, to improve measurement-derived estimates of emissions. These estimates could lead to more accurate emissions reporting, for example through the Scientific Assessment of Ozone Depletion.

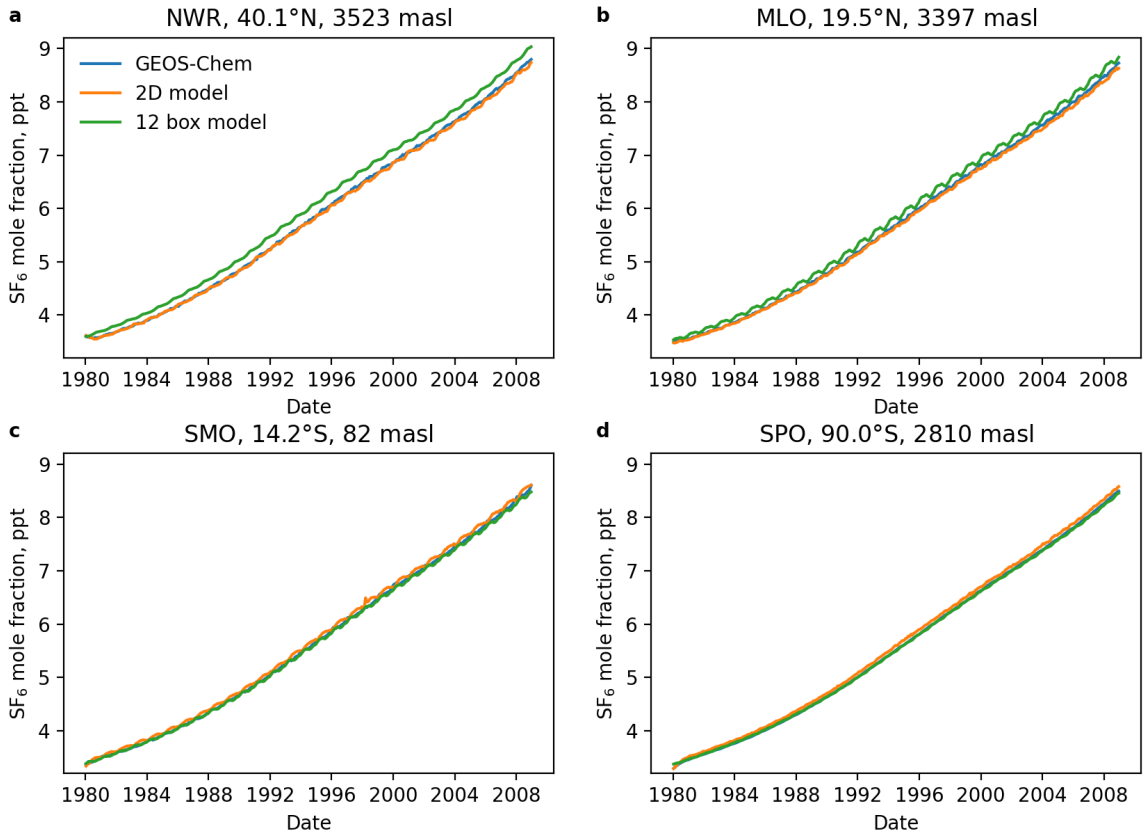

Figure 1. A comparison of the model output of sulfur hexafluoride (SF_6) mole fraction from the 3D transport GEOS-Chem, the new 2D model and a 12-box model at four NOAA site locations.

Unexpected Seasonal Cycle of US Anthropogenic Methane Emissions

L. Hu[1], A.E. Andrews[1], S.A. Montzka[1], S. Ibarra-Espinosa[2], S. Miller[3], N. Miles[4], K. Davis[4,5], Z. Barkley[4], L. Bruhwiler[1], C. Sweeney[1], A. Crotwell[2], K. McKain[1], Y. Oh[2,1], X. Lan[2,1], K. Thoning[1], and M. Madronich[2,1]

[1]NOAA Global Monitoring Laboratory (GML), Boulder, CO 80305; 720-319-7805, E-mail: lei.hu@noaa.gov
[2]Cooperative Institute for Research in Environmental Sciences (CIRES), University of Colorado, Boulder, CO 80309
[3]Stanford University, Stanford, CA 94305
[4]The Pennsylvania State University, Department of Meteorology and Atmospheric Science, University Park, PA 16802
[5]The Pennsylvania State University, Earth and Environmental Systems Institute, University Park, PA 16802

Methane is a major greenhouse gas (GHG) that has contributed to one third of the warming induced by all GHGs since the preindustrial era (IPCC, 2021). Reliable quantification of methane emissions is critical in tracking progress towards methane mitigation, especially over the U.S. where the government has firm plans for reducing its national methane emissions. Atmosphere-based top-down estimates play a vital role in supplying an independent, measurement-based emission estimate that complements the Environmental Protection gency's (EPA) annual GHG inventories with additional temporal information. In this study, we quantified U.S. methane emissions using inverse modeling of ground- and airborne- methane measurements made from the NOAA Greenhouse Gas Reference Network for 2007 – 2021. Our results show an unforeseen seasonal cycle in anthropogenic methane emissions from the U.S. in all model scenarios, where we considered different transport models, different a priori emissions, and different background estimates for all years of our analysis. The derived seasonal emissions were most pronounced in the major natural gas production region and is similar to the seasonal variability of ethane and propane derived for the U.S. Both suggest this season emissions were likely caused by national gas-related activities.

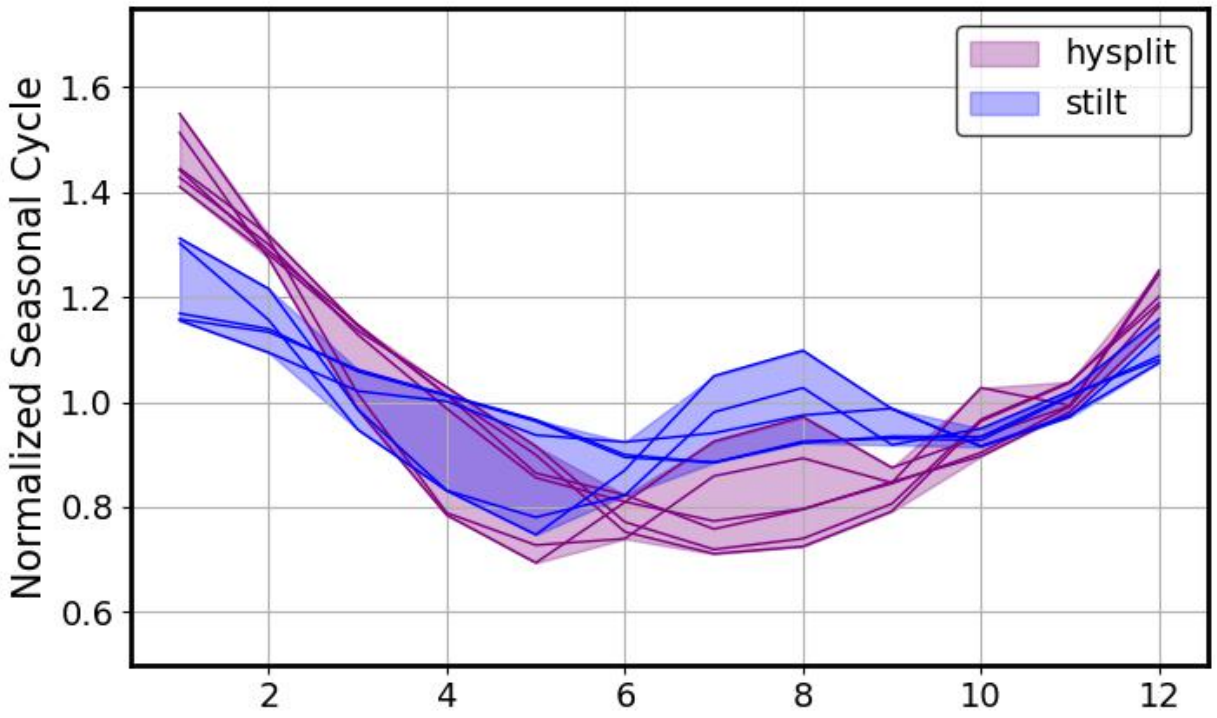

Figure 1. Seasonal cycle of methane derived from atmospheric inverse modeling using whole-air flask measurements from NOAA's Greenhouse Gas Reference Network. Seasonal cycle was calculated by derived monthly emissions normalized by annual emissions and averaged between 2008 and 2017.

Improving Regional Carbon Flux Quantifications with CO_2 Observations from Satellite, Surface, and Aircraft

J. Liu[1], A. Chatterjee[2], V. Payne[1], and The OCO-2/3 Science Team[1]

[1]NASA Jet Propulsion Laboratory, California Institute of Technology, Pasadena, CA 91109; 626-567-6008, E-mail: junjie.liu@jpl.nasa.gov
[2]NASA Goddard Space Flight Center (GSFC), Greenbelt, MD 20771

As climate changes become more severe and many countries pledge to reach carbon neutrality by mid-century, it becomes ever more urgent to improve our understanding of both fossil fuel emissions and natural carbon fluxes using CO_2 observations from all platforms. Satellite CO_2 observations have the advantage of global coverage, but are prone to biases. Surface CO_2 observations are accurate and precise but have limited spatial coverage. CO_2 observations collected with aircrafts are limited in both space and time but provide critical vertical information that surface and satellite observations are lacking. In this presentation, we will focus on the advancement in simultaneous use of CO_2 observations from these platforms to quantify natural carbon fluxes and fossil fuel emissions, with an emphasis on satellite observations from OCO-2/3. Through comparison to surface remote sensing network TCCON, the retrievals from OCO-2/3 are traced to the WMO standard. We will first show the data quality of OCO-2 and OCO-3 observations during their records. We will then showcase the advancements in three aspects: (1) country-scale carbon budget quantification and how the estimate depends on the observation sources; (2) quantification of impact of extreme climate event on carbon fluxes with regional nested-model (Figure 1); and (3) quantification of regional carbon flux uncertainties with aircraft observations. In the end, we will discuss potential future directions to quantify both anthropogenic emissions and natural carbon fluxes by combining observations from all platforms.

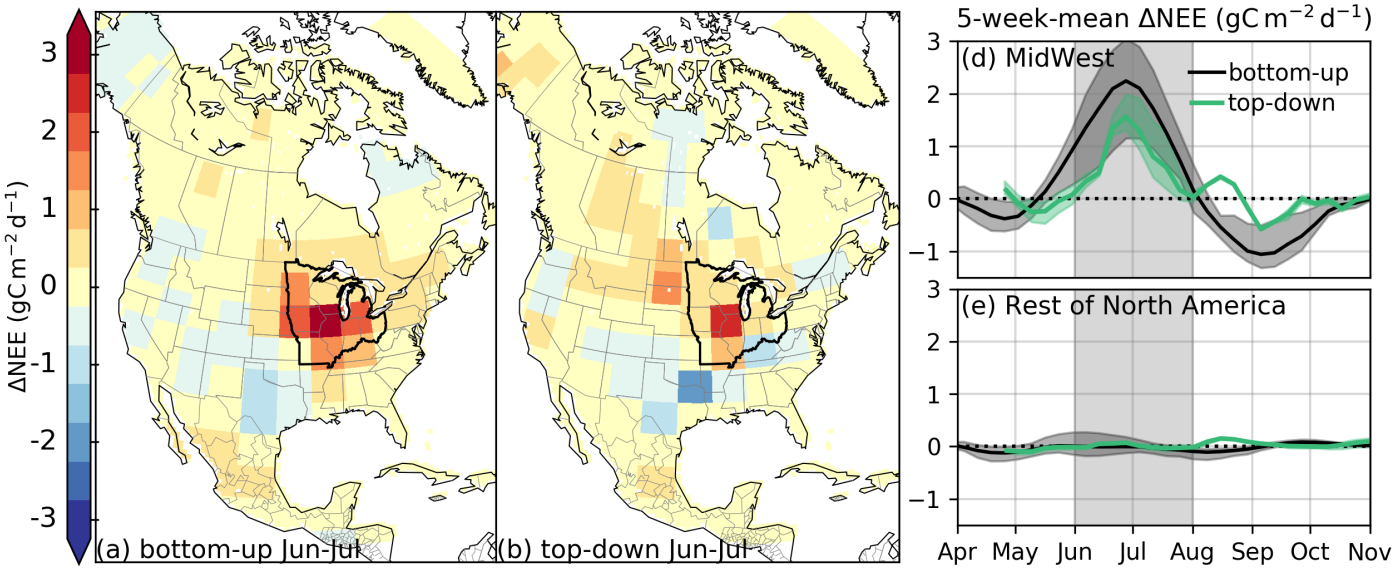

Figure 1. Regional nested-mode inversions better capture flux anomalies caused by extreme flood events in 2020 over mid-west. Left panel: net ecosystem exchange (NEE) anomalies between June-July 2020 inferred from NIRv and SIF observations (unit: gC/m²/day); middle-panel: NEE anomalies between June-July 2020 estimated by a regional nested top-down inversion model; Right panels: monthly NEE anomalies from bottom-up and top-down over the mid west and the rest of north America. (Byrne et al., in preparation).

Using Satellite Observations and Surface Aerosol Monitoring Networks (e.g., BC2 and NFAN) to Characterize Long-range Mineral Dust Transport in the U.S.

M. Mehra[1], S. Shrestha, K. AP, R. Kumar[2], E. Andrews[3,4], J. Sherman[5], J.H.F. III, S. Usenko, and R.J. Sheesley

[1]Baylor University, Waco, TX 76706; 254-400-6290, E-mail: manisha_mehra@baylor.edu
[2]National Center for Atmospheric Research (NCAR), Boulder, CO 80307
[3]Cooperative Institute for Research in Environmental Sciences (CIRES), University of Colorado, Boulder, CO 80309
[4]NOAA Global Monitoring Laboratory (GML), Boulder, CO 80305
[5]Appalachian State University, Department of Physics and Astronomy, Boone, NC 28608

Adopting cleaner technologies for sectors such as transportation, coal-fired power plants, and industry has reduced urban anthropogenic emissions for select pollutants in the United States (U.S.). This change in urban emissions combined with other factors has renewed efforts to understand the impact of biomass burning (BB) and mineral dust on air quality and radiation budget. To address scientific air quality questions about the frequency and seasonality of BB and mineral dust and to estimate the impact on radiative forcing, measurements of aerosol optical properties are made by the (i) Texas Commission on Environmental Quality (TCEQ) Black and Brown Carbon (BC2) network in Texas, US and (ii) National Oceanic and Atmospheric Administration (NOAA) Federated Aerosol Network (NFAN) in different parts of the world. The basic aerosol optical properties measured at the BC2 and NFAN sites include aerosol light scattering (total and backward hemisphere) and light absorption. Here we present a case study of characterizing transport and impacts of June 2020 Saharan dust on the air quality at three different sites: (i) southern U.S. (West Liberty, Houston, Texas; BC2 site), (ii) eastern U.S. (Appalachian State University, Boone, North Carolina; NFAN site), and (iii) midwestern US (Bondville, Illinois; NFAN site). The main aim of this study is (i) to evaluate the feasibility of using aerosol optical properties for near real-time detection of the influence of Saharan dust at sites with different background conditions and, (ii) to estimate the impact of Saharan dust aerosols on the regional radiation budget. The details about the relevance of such a huge Saharan dust event on air quality and its impact on the radiation budget will be discussed during the presentation.

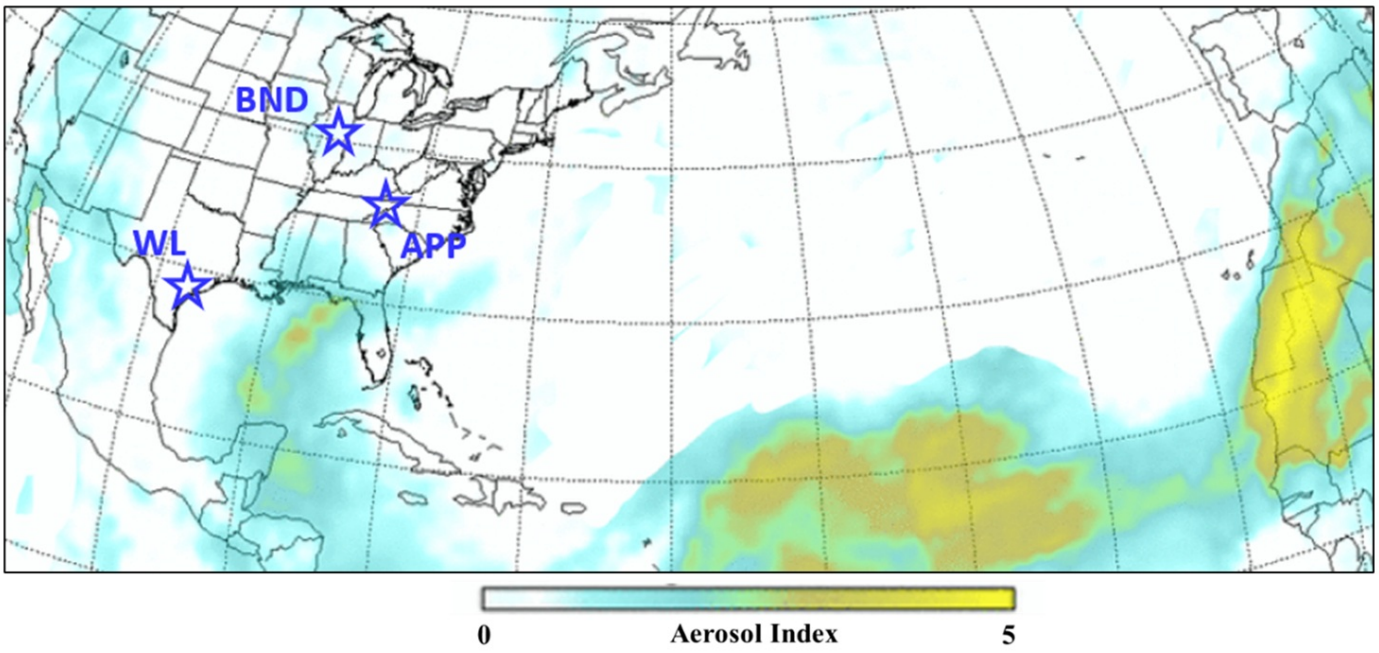

Figure 1. Spatial distribution of average aerosol index [AI] retrieved from Suomi NPP OMPS for June 25 & 26, 2020 *[Source: NASA/NOAA]*. A dense dust plume is observed over the eastern, central Atlantic and the Caribbean Basin with AI above 3. The geographical locations of the BC2 site (WL) and the NFAN monitoring sites (APP and BND) are also shown.

A Long-term Study of Aerosol Concentrations and Solar Radiation at Mt. Lulin (2,862m) in East Asia

H. Huang[1], S. Wang[1], B. Andrews[2,3], C. Ou-Yang[1], Y. Chiu[4], J. Yu[4], C. Huang[4], P. Shieh[4], and N. Lin[1,5]

[1]National Central University, Department of Atmospheric Sciences, Taoyuan, Taiwan; 886-34227151, E-mail: zhai332@gmail.com
[2]Cooperative Institute for Research in Environmental Sciences (CIRES), University of Colorado, Boulder, CO 80309
[3]NOAA Global Monitoring Laboratory (GML), Boulder, CO 80305
[4]Environmental Protection Administration, Department of Environmental Monitoring and Information Management, Taipei City, Taiwan
[5]National Central University, Center for Environmental Monitoring and Technology, Taoyuan, Taiwan

The Lulin Atmospheric Background Station (LABS) located at Mt. Lulin (2862m) in central Taiwan was established to monitor the atmospheric compositions and radiation in the lower free troposphere of East Asia since 2006. The multi-year monitoring of LABS (17-years) will help to understand the climatology of the anthropogenic activity, aerosol optical properties, and radiation variation. To look into the details of this topic, we use aerosol and radiation measurement, including Thermo TEOM, aerosol *in situ* system (i.e. particle soot absorption photometer, continuous light absorption photometer, TSI Nephelometer, and TSI Condensation Particle Counter) operated by NOAA ESRL/GMD, Kipp & Zonen solar instruments (i.e. Pyranometer and Pyrgeometer), to analysis seasonal and interannual variation.

Figure 1 shows that trends in aerosol mass concentrations and extinction coefficient have decreased over 17 years at the LABS. Using the radiative-transfer calculation of cloud-free conditions, the surface short-wave downward (SWD) and long-wave downward (LWD) radiation showed a significant increasing trend. The increasing SWD and decreasing aerosol concentrations matched the direct aerosol effect theory, which illustrates the interannual variation of aerosol will further have climate implications.

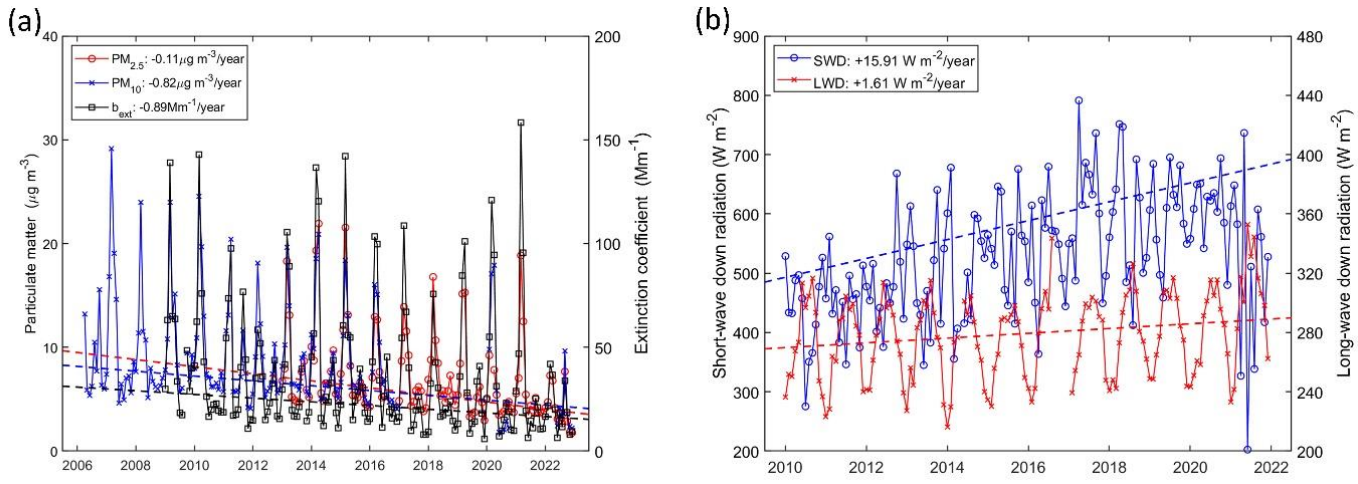

Figure 1. Trends in (a) the aerosol concentrations of particulate matter (PM) and aerosol extinction coefficient (b_{ext}), (b) the surface short-wave downward (SWD) and long-wave downward (LWD) radiation during cloud-free conditions at LABS. The trend analyses were performed using Sen's slope estimator.

Decreasing Aerosol Hygroscopicity at the NOAA FAN Site at Appalachian State University and the Potential Role of Changing Aerosol Composition

J.P. Sherman, P. Liu, and L. Yin

Appalachian State University, Department of Physics and Astronomy, Boone, NC 28608; 724-664-9077, E-mail: shermanjp@appstate.edu

The Southeastern U.S., home to high levels of biogenic secondary organic aerosol and sulfate aerosol loading during summer, is one of only a few regions that did not warm in the 20th century. Aerosol optical depth, lower tropospheric scattering and absorption coefficients have all demonstrated statistically-significantly decreasing trends in the past decade (Collaud-Coen, et al., 2020), likely in response to the large decreases in SO_2 and NO_x emissions in the Eastern U.S. Since sulfate is decreasing faster than organics in the SE U.S. (Hand et al (2014) and Fig.1), aerosol hygroscopicity and its seasonality may also be changing. The NOAA FAN site at Appalachian State University (APP) possesses the longest active, continuous dataset of aerosol light scattering enhancement factor f(RH) in the continental U.S. (2012-present) so studies of changes in aerosol hygroscopicity are now possible. Aerosol chemistry at APP is representative of the background SE U.S. (Link et al., 2015).

This presentation outlines how aerosol hygroscopicity is changing over the past decade at APP, in the context of changing aerosol composition at six regional EPA monitoring sites. The scattering hygroscopic enhancement factor f(RH) experienced a steep decline in 2016 (Fig.2), coincident with increasing organic aerosol concentrations and continued decrease in sulfate in the region (Fig.1). Since 2016, f(RH) has exhibited only small changes, while sulfate mass concentrations have remained relatively constant. Strong positive (negative) correlations were observed between the gamma fit parameter to f(RH) measured at APP and the sulfate and sulfate (organic) mass fractions measured by a collocated quadrupole aerosol mass spectrometer during summers 2012-2013 and the winter in between (Fig.1). This, along with the decreasing sulfate mass concentrations and mass fractions (Fig. 1) suggest that the changing aerosol composition is likely playing a role in the changing aerosol hygroscopicity. Less hygroscopic aerosols will have effects on not only aerosol light scattering but also their ability to serve as cloud condensation nuclei (CCN).

References

Hand, J. L., et al (2014) *Atmos. Environ.*, 94, 671–679

Link, M.F.et al (2015) *J. Atmos. Chem*. 2015, 72, 81-104

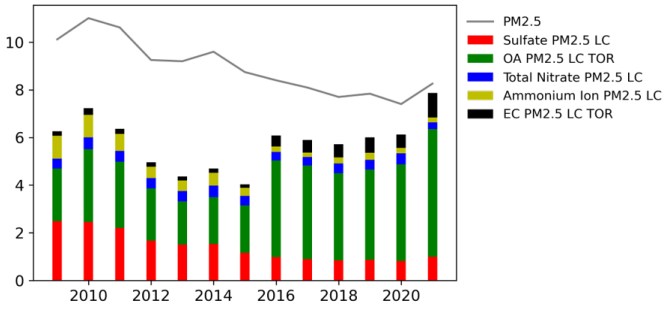

Figure 1. Figure 1. Annual mean speciated $PM_{2.5}$ mass concentrations from six EPA sites near APP.

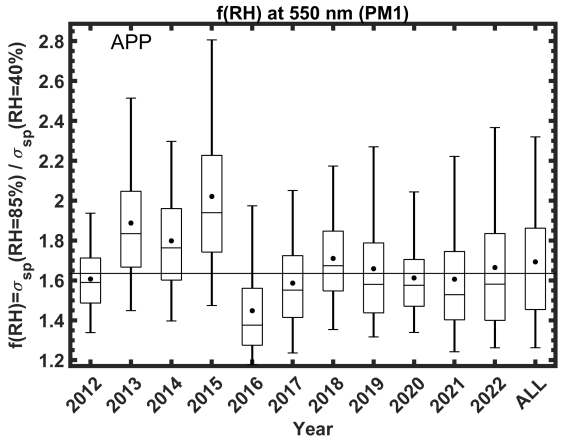

Figure 2. Figure 2. Box plots of aerosol hygroscopic scattering enhancement f(RH) at APP over full years. The 'ALL' box provides the statistics for all days the 2013-2022 period. The mean is denoted by the dot while the horizontal bar represents the median.

Application of BC Observations to Quantify CO and its Contribution from Fossil Fuel and Biomass Burning Fractions over the Central Himalayas

P. Srivastava[1,2], M. Naja[2], R. Kumar[3], P. Bhardwaj[3], and P.T.R. Seshadri

[1]National Institute for Environmental Studies, Tsukuba-City, Ibaraki, Japan; +81298502567, E-mail: srivastava.priyanka@nies.go.jp
[2]Aryabhatta Research Institute for observational sciences (ARIES), Department of Science and Technology (DST), Atmospheric Science Division, Govt. of India, Nainital, Uttarakhand, India
[3]National Center for Atmospheric Research (NCAR), Boulder, CO 80307

The continuous and simultaneous ground-based observations of carbon-based aerosols and trace gases are significantly sparse over the pristine Himalayan region while there are diverse emission sources in its adjacent plain regions. This limits source apportionment studies essential for formulating pollution mitigation and related policies. Thus, in the present work, five years (2014-18) of ground-based observations of equivalent black carbon (eBC) are used for estimating CO mixing ratios and to identify its fossil fuel and biomass emission fraction at a high-altitude (1958 m a.m.s.l) site in the Central Himalayas. CO and eBC observations are used in the multiple linear regression based (MLR) framework and it is shown that MLR does well in replicating the diurnal and monthly variations and is able to estimate CO with an $r^2 > 0.8$ for the training period of 2014 - 2017. MLR predicted CO during 2018 closely follows the observed variations, and its mixing ratios lie within 17% of the observed CO values in any given month. Segregation shows that the CO_{ff} (ff: fossil fuel) has a greater unimodal diurnal amplitude (39.1 to 67.8 ppbv) compared to CO_{bb} (bb: biomass burning) which ranges from 5.7 to 33.5 ppbv. Overall, CO_{ff} is found to be the major contributor (27%) in CO after its background fraction (58%). CO_{bb} fraction is as high as 28% during spring, a period of increased agricultural and forest fires in the Northern Indian region. In comparison, the satellite and model estimates (MOPITT, MERRA2, and WRF-Chem with tracer runs) are unable to reproduce the temporal variations in CO in this region. The results thus highlight the successful applicability of MLR for CO segregation and provide the parameters for future estimation of CO from eBC. The work attempts to address the need to have continuous monitoring of CO and segregate its fossil fuel and biomass source fractions, particularly over the Himalayan area, to aid in the development of mitigation solutions for the region.

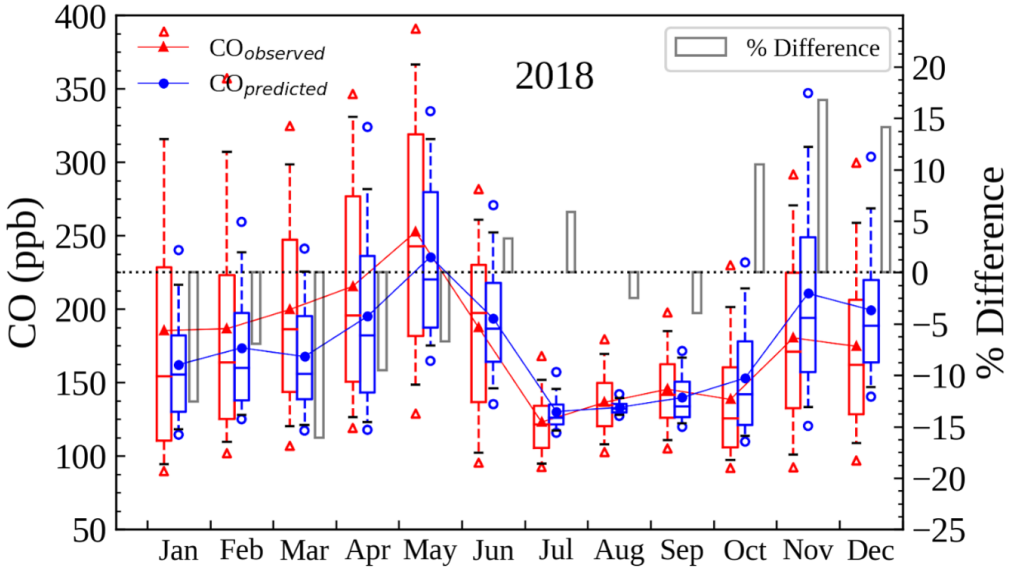

Figure 1. The monthly mean variation in observed CO and predicted CO for the year 2018. In boxplots, the lower and upper edges of the boxes represent the 25th and 75th percentiles, respectively. The whiskers below and above are the 10th and 90th percentiles and the unfilled triangles and circles depict the 5th and 95th percentiles. The solid triangles and circles inside the boxes represent the mean and the solid lines inside the boxes represent the median. The percentage difference between observed and predicted CO for the year 2018 is also shown by grey bars.

Surface Solar Radiation Variability in Complex Cloud-Aerosol Environments: New Insights from Observations and High-Resolution Simulations

J. Gristey[1,2], G. Feingold[2], I.B. Glenn[3], K.S. Schmidt[4], and H. Chen[4]

[1]Cooperative Institute for Research in Environmental Sciences (CIRES), University of Colorado, Boulder, CO 80309; 720-491-1089, E-mail: Jake.J.Gristey@noaa.gov
[2]NOAA Chemical Sciences Laboratory (CSL), Boulder, CO 80305
[3]Joint Institute for Regional Earth System Science and Engineering (JIFRESSE), UCLA, Los Angeles, CA 90095
[4]University of Colorado, Laboratory for Atmospheric and Space Physics (LASP), Boulder, CO 80309

Ubiquitous shallow cumulus clouds exhibit detailed three-dimensional (3D) spatial structure leading to complex variability in surface solar irradiance (SSI). Hygroscopic aerosol embedded in the cloud field introduces additional scattering and absorption, further modulating SSI. The SSI variability in this environment is encapsulated by the shape of the SSI probability density function (PDF), which is typically bi-modal representing separately the cloud shadows and the gaps between (e.g., Fig. 1a). However, detailed understanding of the relationship between cloud and aerosol properties, and the SSI PDF shape, has remained elusive. Here, we compare observations of SSI at the Southern Great Plains Atmospheric Observatory in Oklahoma, with simulated SSI derived from large eddy simulation and Monte-Carlo 3D radiative transfer for a variety of shallow cumulus cases. First, this presentation will reveal the stark differences between simulated SSI when 3D radiative effects are included or neglected (e.g., Fig. 1b). The observed SSI PDF shape is only reproduced when 3D radiative effects are included, providing direct observational evidence for 3D radiative effects. Next, a machine learning framework will be introduced for predicting the SSI PDF using just a handful of key cloud and aerosol properties. It will be demonstrated how well the SSI PDF can be predicted relative to traditional 1D radiative transfer, while bypassing the computational expense of 3D radiative transfer. Finally, machine learning inference techniques will be described that permit quantification of the relative importance of each predictor and aid in the understanding of physical controls on SSI variability, thereby uncovering the key role of aerosol embedded in the cloud field. The new findings have important implications for solar renewable energy assessment and highlight the potential significance of shortwave 3D radiative effects in atmospheric modeling. Opportunities and challenges for future parameterization of shortwave 3D radiative effects in high-resolution atmospheric models will be discussed.

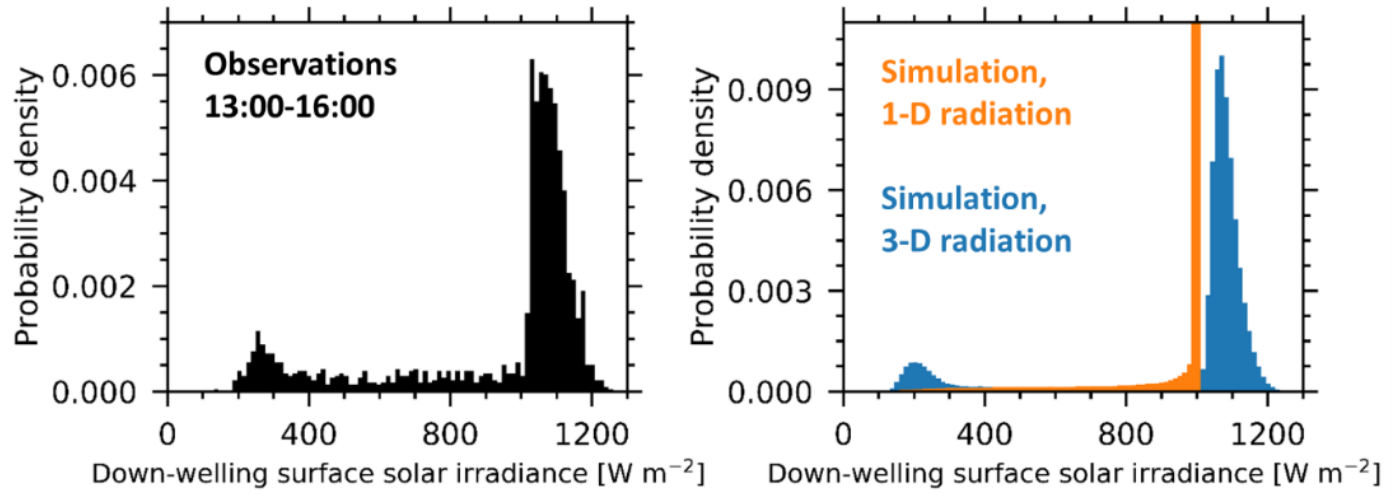

Figure 1. Probability density functions of down-welling surface solar irradiance at the Southern Great Plains atmospheric observatory on June 27 2015 from 13:00-16:00 local time, based on (a) observations and (b) large eddy simulation employing 1-D (orange) and 3-D (blue) radiative transfer.

Updates to the Operational UV Index – Validation Against GRAD Observations

C.S. Long[1], H. Lee[2], and L.M. Ciasto[2]

[1]Retired from the NOAA National Weather Service, National Centers for Environmental Prediction, Climate Prediction Center, College Park, MD 20740; 410-627-2139, E-mail: craig.s.long@gmail.com
[2]NOAA National Weather Service, National Centers for Environmental Prediction, Climate Prediction Center, College Park, MD 20740

The current version of the UV Index forecast system was implemented in 2005. The forecast system makes use of NCEP forecasts of total ozone, cloud transmission in the UV part of the spectrum, and the surface albedo in the presence of snow. At that time there was no forecast of tropospheric aerosols, so an aerosol climatology is used. Validation of the UV Index using GRAD observations showed that the forecasts overestimated the surface UV when wild fire smoke or African dust were present. In the last couple years NCEP has been working on producing operational aerosol forecasts resulting in greater location and accuracy than using any climatology. CPC has been testing the use of these aerosol forecasts in the UV Index forecasts with significant improvements even in areas not impacted by smoke or dust. Other improvements (0.25° grid output spacing, using hourly vs 3 hourly radiation forecasts) will also be put in place. The validation exercises also helped to identify problems in the ground observation networks (calibration, maintenance, etc) that were otherwise unnoticed. This presentation will highlight all the improvements to the UV Index forecast system with emphasis on the aerosol contribution.

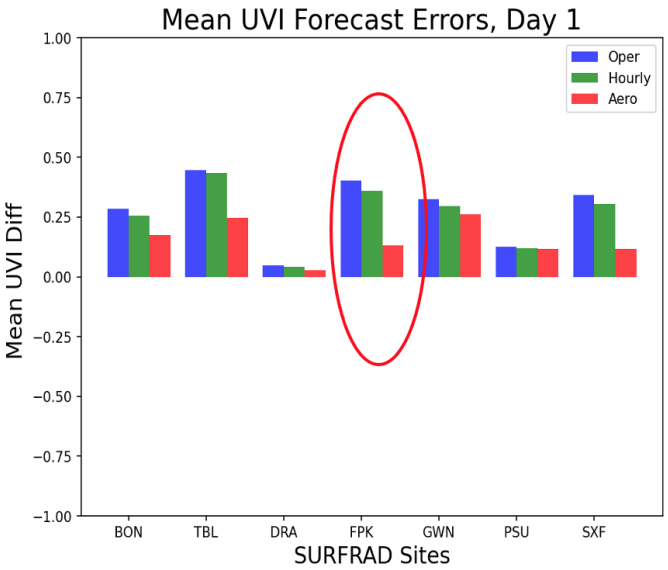

Figure 1.

UVI Day-1 Forecast Bias at the SURFRAD sites, assessed for the Operational (blue), Hourly (green), Hourly+GEFS_Aerosol (red) models, with all hourly data over the period Jul2021-Jun2022**.** Note that the forecasts with aerosols decreased the UVI forecast errors particularly at Fort Peck where smoke from wild fires impacted the observations.

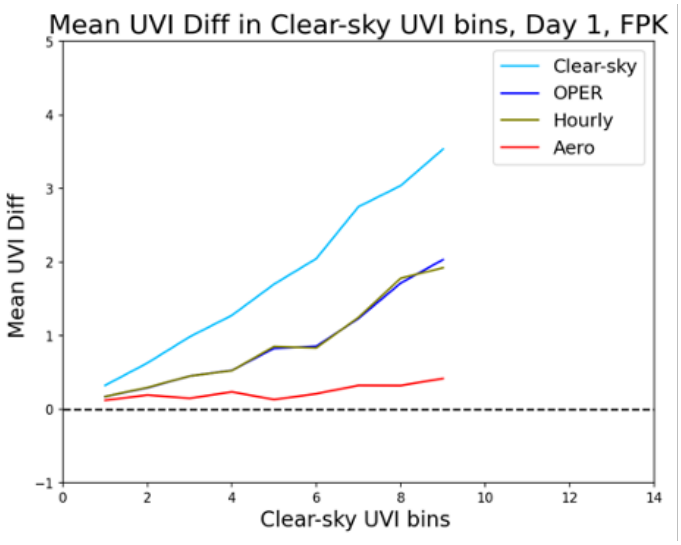

Figure 2.

The UVI Forecast bias errors are stratified by the clear-sky UVI to homogenize the assessment bases. The UVI Forecast Biases for v2.0.0 (”Aero”, red) at Fort Peck is clearly seen to be significantly reduced from the current model (“OPER”, blue) and are more uniformly distributed over clear-sky bins.

Linking Atmospheric Data to High-quality Gas Standards – a 25+ Year Perspective

B. Hall[1], A. Crotwell[2,1], D. Kitzis[2,1], S.A. Montzka[1], I. Vimont[2,1], T.K. Mefford[2,1], and S. Clingan[2]

[1]NOAA Global Monitoring Laboratory (GML), Boulder, CO 80305; 303-497-7011, E-mail: Bradley.Hall@noaa.gov
[2]Cooperative Institute for Research in Environmental Sciences (CIRES), University of Colorado, Boulder, CO 80309

A key component of GML's research involves the ability to prepare in-house gas standards, both to establish calibration scales, and for use as working standards for various measurement programs. The ability to link measurements made by different instruments across a variety of spatial and temporal scales is one of the strengths of GML's measurement programs, and provides the basis for our role as a WMO Global Atmospheric Watch (GAW) Central Calibration Laboratory. Having the ability to make custom gas standards also gives us the ability to efficiently test for artifacts, such as co-elution in gas chromatography, and matrix effects in other analytical techniques. Over the last 25+ years, we have utilized and developed various methods to prepare gas standards using gravimetric and manometric methods, which tie many atmospheric measurements to common well-defined scales. Along the way, we have made improvements in the laboratory, in analytical systems, in data management, and in the preparation of natural air standards in response to new measurement challenges. This presentation will highlight some of the successes and challenges over the last few decades.

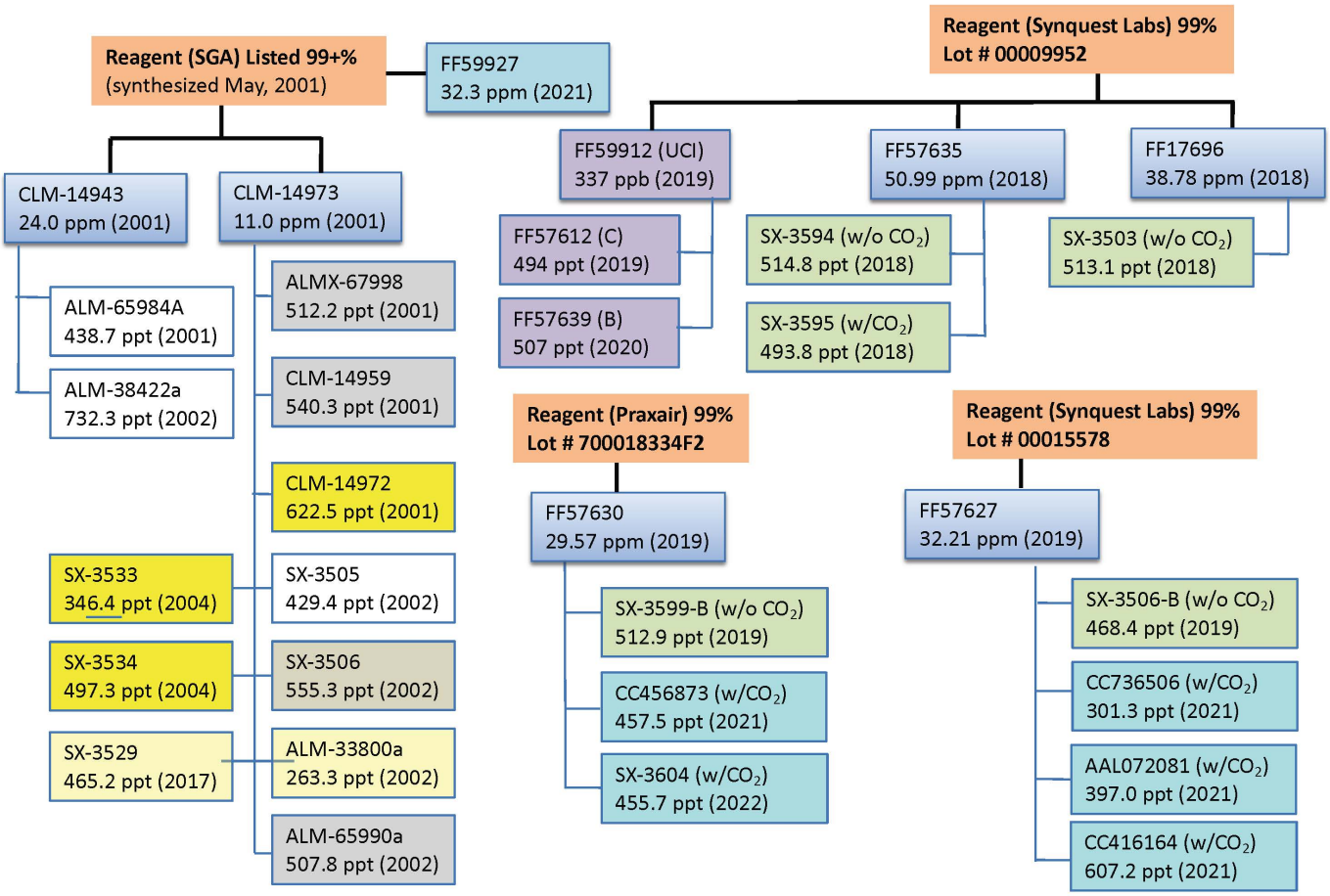

Figure 1. History of carbonyl sulfide standards prepared since 2001.

Improving Data Quality in Long-term Canadian Ozone Sounding Records

D.W. Tarasick[1], R.M. Stauffer[2], H.G.J. Smit[3], A.M. Thompson[2], J. Davies, R. Van Malderen[4], B.J. Johnson[5], H. Vömel[6], and D.E. Kollonige[2,7]

[1]Environment and Climate Change Canada (ECCC), Toronto, Ontario, Canada; 437-580-3243, E-mail: david.tarasick@ec.gc.ca
[2]NASA Goddard Space Flight Center (GSFC), Atmospheric Chemistry and Dynamics Laboratory, Greenbelt, MD 20771
[3]Institute for Energy and Climate Research, Troposphere IEK-8, Research Center Juelich, Juelich, Germany
[4]Royal Meteorological Institute of Belgium, Brussels, Belgium
[5]NOAA Global Monitoring Laboratory (GML), Boulder, CO 80305
[6]National Center for Atmospheric Research (NCAR), Boulder, CO 80307
[7]Science Systems and Applications, Inc. (SSAI), Lanham, MD 20706

An abrupt change in ozone bias relative to several satellite sensors --a total column ozone (TCO) “dropoff” of about 2-3% –has been reported at number of ozonesonde stations (Stauffer et al., 2020), including Canadian stations. The dropoff affects stratospheric measurements from the EnSci ozonesonde, after about 2013 (approximately serial number 25000). Corrections and additional data have reduced the estimated dropoff at most Canadian sites (Stauffer et al., 2022). The Canadian network recently switched to Science Pump sondes (after serial number 32000), and this has reversed the dropoff, and approximately restored agreement with satellite sensors.

It is not standard practice to calibrate individual ozonesonde pumps before launch, as this is difficult and labour-intensive; rather an average pump calibration is used in data processing. Recently, an analysis of an extensive record of individual EnSci pump calibrations made since 2009 (Nakano and Morofuji, 2023) has shown a small negative shift, after serial number 25000, in the low-pressure pump correction. This systematic shift agrees well with the average differences found with MLS for Canadian EnSci data between 100 hPa and 10 hPa, both in magnitude and in variation with altitude.

The use of these new pump corrections with Canadian data is explored, and results are compared to MLS, and other satellite sensors. The correction for the change in pump efficiency reduces or removes the dropoff in the time series of satellite comparisons; when serial number 25000 is chosen as a breakpoint, the step changes over 7 stations and four satellite sensors (GOME2a, GOME2b, OMI, OMPS) vary between +2.4% and -3.1%, with an average of -0.6%. In contrast, the average change with the recent switch to Science Pump sondes is +1.9% (based on a limited number of flights).

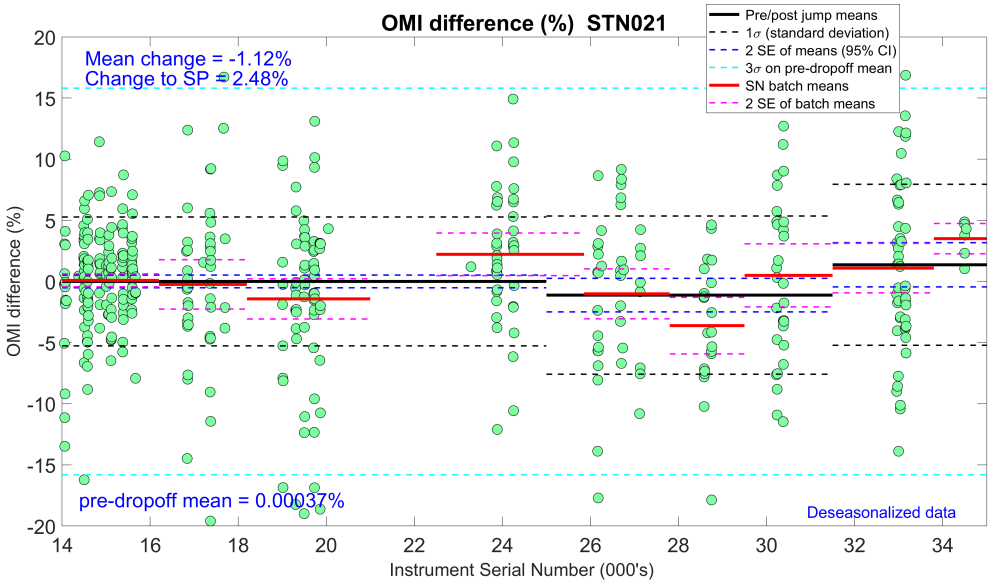

Figure 1. Comparison of sonde integrated ozone and OMI overpass data at Edmonton, 2010-2022.

Arctic Stratospheric Measurements of Aerosol, Water Vapor, and Ozone during SABRE

E.C. Asher[1,2], A. Baron, P. Cullis[2], T. Thornberry[3], B.J. Johnson[2], E.G. Hall[2], R. Gao[3], D.F. Hurst[1,2], and G.A. Morris[4]

[1]Cooperative Institute for Research in Environmental Sciences (CIRES), University of Colorado, Boulder, CO 80309; 512-587-2684, E-mail: elizabeth.asher@noaa.gov
[2]NOAA Global Monitoring Laboratory (GML), Boulder, CO 80305
[3]NOAA Chemical Sciences Laboratory (CSL), Boulder, CO 80305
[4]St. Edward's University, Austin, TX 78704

Water vapor mixing ratios and aerosol number concentration and size can affect polar stratospheric ozone chemistry. To date, however, the number of *in situ* measurements of aerosol or water vapor at high latitudes and high altitudes in the Northern Hemisphere (NH) are limited. These observations constrain global climate model simulations and are critical for the evaluation and improvement of satellite retrievals in this region. The Stratospheric Aerosol processes, Budget and Radiative Effects (SABRE) mission between February and March 2023 was designed, in part, to address these issues. In conjunction with SABRE, our team flew four Baseline Balloon Stratospheric Aerosol Profiles-Intensive Operation Period (B^2SAP-IOP) payloads on weather balloons from near the Barrow Atmospheric Baseline Observatory in Utqiagvik, AK between March 13 and March 20, 2023. These payloads carried a combination of aerosol sondes, NOAA frost point hygrometers, and ozonesondes to ~ 28 km altitude and were timed to overlap with high-altitude WB-57 research aircraft flights (to ~ 16 km altitude) over Utqiagvik, AK.

Our balloon-borne observations showed that ozone mixing ratios and air temperature varied considerably between 15 – 25 km across the edge of the polar vortex. Corresponding water vapor mixing ratios increased gradually from ~5 ppmv to ~7 ppmv with altitude above 15 km, agreeing well with Aura Microwave Limb Sounder (MLS) retrievals. Meanwhile, aerosol number concentrations steadily decreased with altitude in the polar stratosphere. We observed enhancements in aerosol surface area above the tropopause and enhancements in aerosol number concentration at ~25 km, likely related to the transport (and dilution) of the Hunga Tonga-Hunga Haʻapai plume, and the descent of meteoric material descending through the upper branch of Brewer-Dobson circulation, respectively. Overall, these findings provide valuable insights into the current baseline state and variability of polar stratospheric composition, chemistry and dynamics.

Figure 1. Launch from Utqiagvik, AK on March 14th, 2023. Photo by Patrick Cullis.

Preliminary Balloon-borne in Situ Water Vapor Intercomparison from Aire-sur-l'Adour, France: September 2022

E. Hall[1], D. Hurst[2,1], M. Ghysels, and N. Amarouche

[1]NOAA Global Monitoring Laboratory (GML), Boulder, CO 80305; 720-739-0097, E-mail: emrys.hall@noaa.gov
[2]Cooperative Institute for Research in Environmental Sciences (CIRES), University of Colorado, Boulder, CO 80309

Water vapor is Earth's most abundant greenhouse gas and is responsible for about half of Earth's greenhouse effect. Slight variations in the abundance of water vapor in the stratosphere can significantly affect the Earth's radiation budget. Monitoring the abundance of stratospheric water vapor is a crucial aspect of detecting and predicting climate change, as it serves as a significant driver of decadal global surface climate change. In the lower stratosphere, water vapor mixing ratios are less than 10 ppmv. Making accurate measurements of water vapor in the upper troposphere and lower stratosphere remain challenging and few in situ instruments are able to accurately perform this task. For this reason, it is important to have rigorous intercomparisons with stratospheric water vapor instruments with good spatial and temporal matching.

In September 2022, several lightweight hygrometers were flown on different balloons during a one-week intensive intercomparison that took place in Aire-sur-l'Adour, France. The newly developed mid-infrared hygrometer, known as "Pico-Light H_2O," was compared with the NOAA frost point hygrometer (FPH) on three nighttime flights. Two separate Pico-Light instruments were flown on the final night providing an intercomparison between two Pico-Light instruments and the NOAA FPH. The differences were less than 1 ppmv (10%) between 14-22 km. This campaign took place within the framework of the E.U. funded HEMERA project. We also evaluate the performance of the Meteomodem M20 and InterMet Systems iMet-4 radiosondes flown during the campaign with the NOAA FPH.

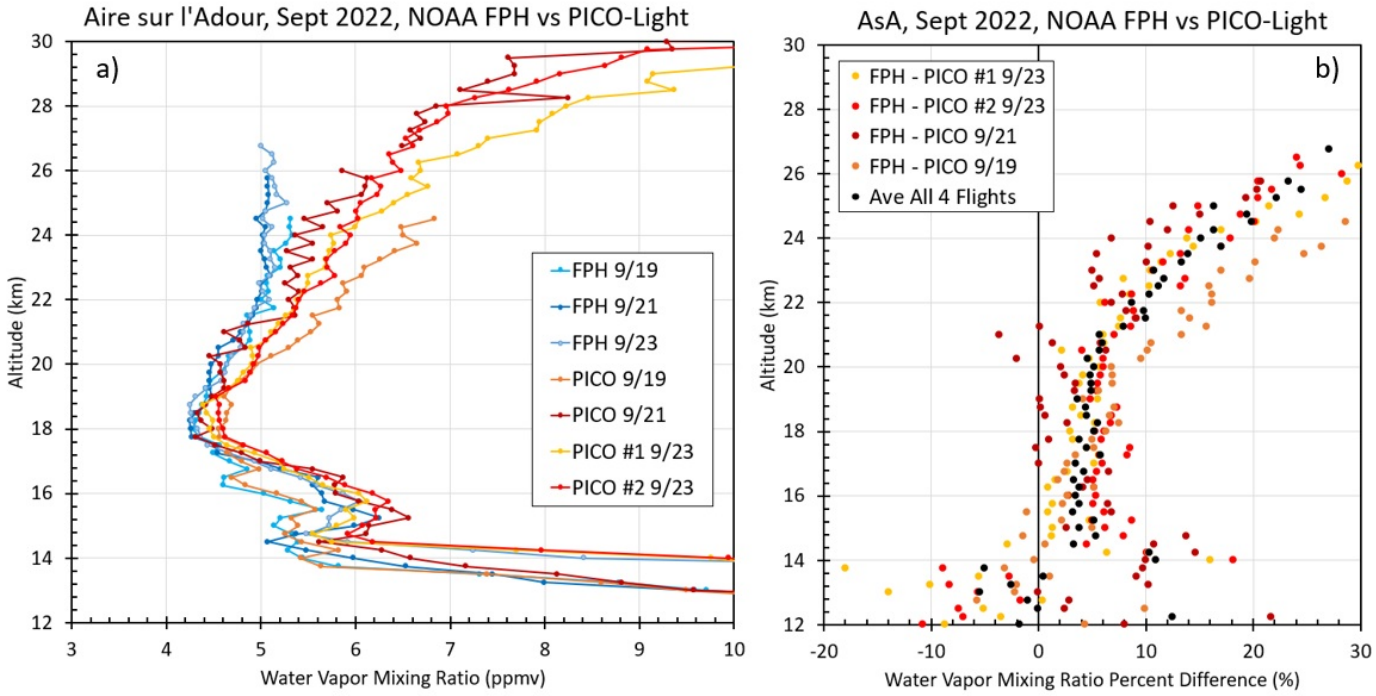

Figure 1. Stratospheric water vapor profiles are shown in panel a) from three-night flights in Aire-sur-l'Adour, France. The percent differences are shown in panel b). Two different Pico-Light instruments were flown on September 23, 2023 launched minutes apart.

TR2Ex Measurements of the Hunga Tonga-Hunga Ha'apai Eruption Plume

P.J. Walter[1], S.L. Alvarez[2], J. Flynn[2], S. Evan[3], J. Brioude[4,5], J. Metzger[6], A. Baron[3,5], G. Payen[7], V. Duflot[3], E.C. Asher[4,8], M.A. Todt[4,5], K.H. Rosenlof[5], T. Thornberry[5], and R. Gao[5]

[1]St. Edward's University, Austin, TX 78704; 512-637-5636, E-mail: pauljw@stedwards.edu
[2]University of Houston, Department of Earth and Atmospheric Sciences, Houston, TX 77004
[3]Laboratoire de l'Atmosphère et Cyclones LACy, UMR8105, Université de La Réunion, 97744 Saint-Denis Cedex 09, France
[4]Cooperative Institute for Research in Environmental Sciences (CIRES), University of Colorado, Boulder, CO 80309
[5]NOAA Chemical Sciences Laboratory (CSL), Boulder, CO 80305
[6]Observatoire des Sciences de l'Univers OSU-Réunion / UMS3365, Université de La Réunion, CNRS, France
[7]UAR 3365 – OSU Réunion, Université de La Réunion, Saint-Denis, Réunion, France
[8]NOAA Global Monitoring Laboratory (GML), Boulder, CO 80305

The 15 January 2022 Hunga Tonga-Hunga Haʿapai (HTHH) eruption led to the Tonga volcano Rapid Response Experiment (TR2Ex) deployment to the Maïdo Observatory in La Réunion (21°S, 55°E). From 21 to 25 January 2022, a suite of balloon-borne in situ stratospheric measurements included sulfur dioxide (SO2), aerosol, ozone, and water vapor complemented by remote sensing observations from ground-based lidar. Four balloon soundings measuring SO2 passed through the HTHH eruption plume at altitudes ranging from 19 to 30 km. The balloon-based in situ SO2 measurements of the HTHH volcanic plume were the first of their kind for a stratospheric volcanic eruption. The first two soundings on 21-22 January occurred in a dense water vapor-rich part of the HTHH plume and had lower SO2 to aerosol extinction ratios than the last two profiles on 24-25 January. Profiles on 21-22 January showed ozone depletion in the HTHH plume, with less than 10% of the observed decrease in ozone signal due to SO2 interference.

References

[1] Yoon, S., Kotsakis, A., Alvarez, S. L., Spychala, M. G., Klovenski, E., Walter, P., Morris, G., Corrales, E., Alan, A., Diaz, J. A., and Flynn, J. H. (2022). Development and testing of a novel sulfur dioxide sonde. Atmospheric Measurement Techniques, 15(14), 4373-4384. https://doi.org/10.5194/amt-15-4373-2022

Acknowledgements

Funding for the SO2 sonde deployment to La Réunion was provided by SilverLining. We thank Maïdo Observatory in La Réunion for hosting members of the Tonga volcano Rapid Response Experiment (TR2Ex).

Stratospheric Ozone Vertical Distribution at Select NOAA Global Monitoring Laboratory Dobson Monitoring Stations and Updated Trends of the Based on the LOTUS Regression Model

J.D. Wild[1,2], I. Petropavlovskikh[3,4], P. Effertz[3,4], K. Miyagawa[5], S. Strahan[6], L. Flynn[7], E. Beach[7], G. McConville[3,4], B.J. Johnson[4], G. Ancellet[8], R. Querel[9], and R. Stübi[10]

[1]Earth System Science Interdisciplinary Center, University of Maryland, College Park, MD 20740; 443-878-4137, E-mail: jeannette.wild@noaa.gov
[2]NOAA Center for Satellite Applications and Research (STAR), College Park, MD 20740
[3]Cooperative Institute for Research in Environmental Sciences (CIRES), University of Colorado, Boulder, CO 80309
[4]NOAA Global Monitoring Laboratory (GML), Boulder, CO 80305
[5]Guest Scientist at NOAA Global Monitoring Division (GML), Boulder, CO 80305
[6]NASA Goddard Space Flight Center (GSFC), Universities Space Research Association (USRA), Greenbelt, MD 20771
[7]NOAA National Environmental Satellite, Data, and Information Service (NESDIS), Camp Springs, MD 20746
[8]LATMOS, Université Pierre et Marie Curie and Centre National de la Recherche Scientifique (CNRS), Paris, France
[9]National Institute of Water and Atmospheric Research (NIWA), Wellington, New Zealand
[10]Federal Office of Meteorology and Climatology, MeteoSwiss

NOAA's ground-based (GB) remote sensing and *in situ* instruments continuously track stratospheric ozone recovery in response to the Montreal Protocol and its amendments. Long-term records of daily Dobson total column ozone, daily Dobson/Umkehr vertical ozone distribution (with a recent new homogenization), and weekly ozonesonde profiles are well-calibrated. Regular intra-instrument comparisons aid in the tracking of instrumental changes. Additionally, NOAA's homogenized satellite record (COH) from SBUV, SBUV/2 and OMPS provides information on ozone vertical distribution in zonal averages allowing the study of large-scale ozone variability. Overpass datasets provide further GB validation including verification of the homogenization of the GB records. The NOAA AC4 funded project assesses the consistency of the trends derived from the different records. We present an updated evaluation of stratospheric ozone profile trends from the long-term ozone record with focus on the 2000–2020 period. Analyses were performed using the updated version (0.8.0) of the Long-term Ozone Trends and Uncertainties in the Stratosphere (LOTUS) Independent Linear Trend regression model. We primarily focus on Boulder, Colorado (40.0N, 105.3W), Haute Provence, France (43.9N, 5.8E), Lauder, New Zealand (45.04S, 169.68E), and Mauna Loa and Hilo, Hawaii (19.5N, 155.58W) which have both sonde and Umkehr measurements, and other stations of opportunity (i.e. Arosa, Switzerland (46.8N, 9.68E).

The Northern Hemispheric sites of Arosa, Haute Provence, and Mauna Loa all show positive trends in the mid to upper Stratosphere with trends peaking at ~3%/decade. Trends in the upper stratosphere at Boulder and Lauder are positive, but not statistically significant. In the lower stratosphere, trends are mostly negative, but trend uncertainties here are quite large. The causes of differences in ozonesonde trends at Lauder and OHP as compared to other datasets are being explored.

We also investigate additional dynamical proxies (Equivalent Latitude, Tropopause Pressure, additional QBO components for example) in the LOTUS model at these sites. We will discuss the addition of these proxies and the impact on the trends and uncertainties.

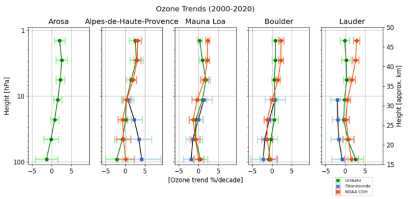

Figure 1. LOTUS trends at five stations with GB and overpass data.

Challenges and Opportunities in Advancing Speciated Characterization of Atmospheric Organics

E.B. Franklin[1,2], L. Yee[3], A. Goldstein[3], and D. Farmer[4]

[1]Colorado State University, Fort Collins, CO 80523; 303-551-3812, E-mail: emily.franklin@colostate.edu
[2]University of California at Berkeley, Berkeley, CA 94720
[3]University of California at Berkeley, Department of Environmental Science, Policy, and Management, Berkeley, CA 94720
[4]Colorado State University, Department of Chemistry, Fort Collins, CO 80523

The composition of atmospheric organics ranging from volatiles to aerosol are incredibly complex, spanning an estimated hundreds of thousands of unique chemical products. Relatively few of these compounds have been structurally identified and catalogued in mass spectral databases. While some properties of this complex organic material can be characterized by bulk analysis, speciated analysis, in particular structure-specific speciated analysis, remains critical for mechanistically probing atmospherically relevant aerosol formation and oxidation processes. Analyzing the speciated composition of highly complex organic mixtures, especially when most separated species cannot be identified, poses both instrumental and analytical challenges. This results in underutilization of the full scope of information made available by advances in instrumentation. This underutilization biases our understanding of the complexity of ambient aerosol formation dynamics, skewing analysis away from complex source groups in which mass is distributed among a larger number of individual contributors. Increased use of data science and machine learning-based techniques has the potential to advance speciated characterization of the atmosphere across environments without depending on synthesis of new products for structural confirmation. From remote forested environments to megacities, cataloging unidentifiable organics throughout the globe has the capacity to streamline identification of key process-specific tracers that currently lie beyond our boundaries of knowledge. Newly developed machine learning-based models allow us to place unidentifiable compounds in chemical property spaces commonly used throughout the atmospheric chemistry community, a process which provides critical context for designing targeted chamber experiments and highlights chemically distinct populations of products that lie beyond the current bounds of knowledge.

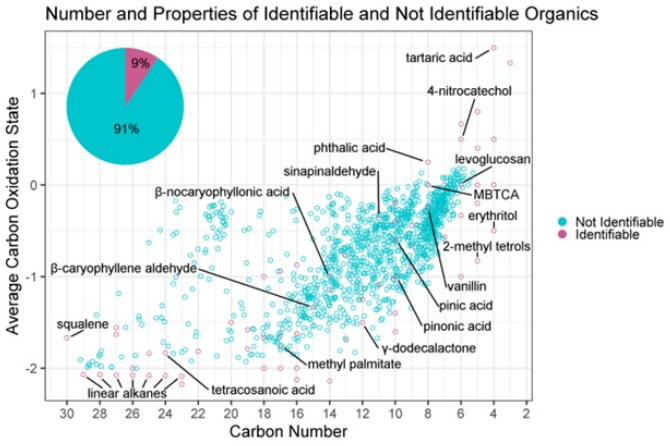

Figure 1. Chemical properties distributions in carbon number- average carbon oxidation state space of identifiable (pink) and not identifiable (teal) organic compounds identified in submicron aerosol collected at the GoAmazon field campaign. Identifiable compounds of interest are labelled in black. The percentage of identifiable and not identifiable compounds compared to the 1325 traced is illustrated by the pie chart in the top right. Carbon numbers of not identifiable compounds are predicted by the Ch3MS-RF model on a continuous scale and predicted carbon numbers are therefore not restricted to integer values.

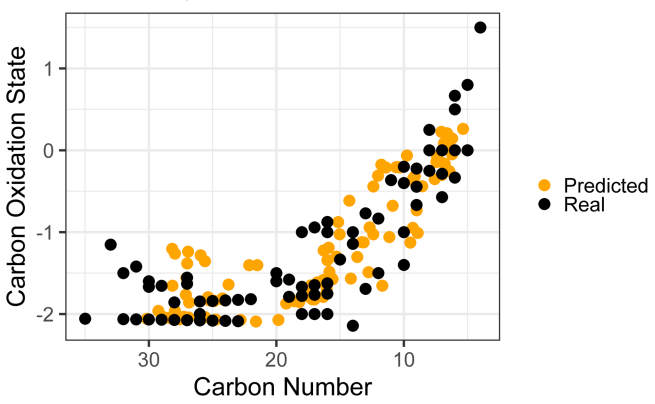

Figure 2. True versus predicted chemical properties distribution of identifiable organic species isolated from aerosol collected at the GoAmazon field campaign within a carbon number - average carbon oxidation state space. True properties are illustrated in black and properties predicted by the Ch3MS-RF model are illustrated in orange.

Applications of Ethane to Methane Ratios: Identifying Abnormal Tank Emissions in the Permian Basin and Implications for Source Apportionment

D. Caulton[1,1], P.D. Gurav[1], A.M. Robertson[1], K. Pozsonyi[1], S. Murphy[1], and D.R. Lyon[2]

[1]University of Wyoming, Laramie, WY 82071; 307-766-5363, E-mail: dcaulton@uwyo.edu
[2]Environmental Defense Fund, Austin, TX 78701

There has been increasing interest in quantifying methane (CH_4) emissions from a view towards mitigation. Properly assessing which sources are emitting is an enduring challenge for the emission quantification community. The use of tracer species to identify particular sources is a promising avenue, however, our understanding of how tracers such as ethane (C_2H_6) vary within source categories is often limited. Lack of observational data and/or data that is not collected directly at the source are common limitations. Here, we present observations of molar ethane to methane ratios (EMRs) for different oil and natural gas (ONG) components in the Permian Basin.

Ground-based sampling of oil and gas production sites in the Permian Basin was carried out in January and October 2020. The 100 EMR observations were not normally distributed (Fig. 1) leading to three statistics that could be used for source attribution: median 14 (±1)%, arithmetic mean 27 (±6)%, and geometric mean 18 (±2)%. We compared these statistics to a regional regression of background CH_4 and C_2H_6 and found that the geometric mean best represented the data. Using the correct statistic is critical for tracer-based attribution methodology.

Source specific EMRs showed that sites where emissions were attributed to a tank produced much higher EMRs averaging 47%. Sites with other noticeable sources such as compressors, pneumatics, and separators had lower and less variable EMRs. Tanks displayed distinct behavior with EMRs between 10-21% producing CH_4 emissions >30x higher than tanks with EMRs >21%. This observation supports the hypothesis that high emission rate tank sources are often caused by separator malfunctions that leak produced gas through liquids storage tanks.

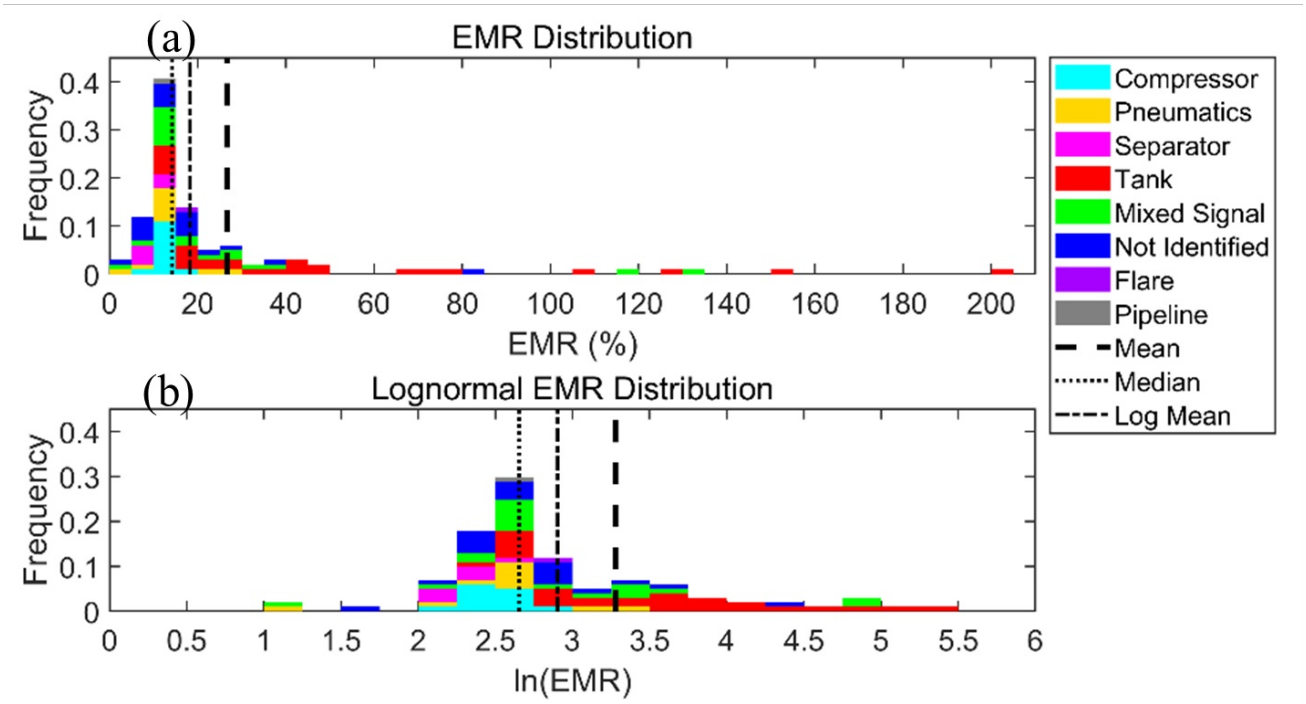

Figure 1. Figure 1. EMR distribution

Distribution of EMRs on (a) normal and (b) lognormal axes. Colors represent the contribution to each bin from the specific source type. Also shown are the arithmetic mean (black dash), median (black dot) and geometric mean (black dot/dash) lines.

Dynamical Drivers of Free-Tropospheric Ozone Increases Over Southeast Asia

R.M. Stauffer[1], A.M. Thompson[1], D.E. Kollonige[1,2], N. Komala[3], H.K. Al-Ghazali, D.Y. Risdianto, A. Dindang, A.F.B. Jamaluddin, M.K. Sammathuria, N.B. Zakaria, B.J. Johnson[4], and P.D. Cullis[4]

[1]NASA Goddard Space Flight Center (GSFC), Atmospheric Chemistry and Dynamics Laboratory, Greenbelt, MD 20771; 717-222-1581, E-mail: ryan.m.stauffer@nasa.gov
[2]Science Systems and Applications, Inc. (SSAI), Lanham, MD 20706
[3]Indonesian Institute of Aeronautics and Space (LAPAN), Jakarta, Indonesia
[4]NOAA Global Monitoring Laboratory (GML), Boulder, CO 80305

Positive trends in tropical free-tropospheric (FT) ozone are frequently ascribed to population and thus emissions growth, but less is known about the effects of changing dynamics and the possible fingerprints of climate change. In an update of our previous work (Thompson et al., 2021; JGR; https://doi.org/10.1029/2021JD034691; "T21"), we re-examine Southern Hemisphere Additional Ozonesondes (SHADOZ) ozone trends over tropical Southeast Asia, one of the most convectively active regions on Earth, now with 25 years of ozone profile data from 1998-2022. T21 posited that consistent, early-year positive FT ozone trends at several tropical SHADOZ stations may be related to decreases in convective activity. Our 25-year analysis of Kuala Lumpur and Watukosek (Java) SHADOZ stations finds that the +5 to +15% (+2 to +6 ppbv) per decade FT ozone trends from ~February-May (Figure 1a) are coincident with large increases in satellite infrared (IR) brightness temperatures (T_b; 1b) and outgoing longwave radiation (OLR; 1d; both are indicators of convective activity), and decreases in convective precipitation amount from NASA's MERRA-2 reanalysis (1c). Trends in ozone and dynamical indicators are generally weak throughout the rest of the year. All of these results suggest that dynamical influences, i.e., decreases in the intensity and frequency of convection, are a primary driver of FT ozone buildup in the early months of the year over Southeast Asia, with waning convection suppressing the typical lofting and redistribution of low, near-surface ozone throughout the tropical FT. The decrease in convective precipitation amounts likely also enables the accumulation of biomass burning emissions, as the Atmospheric Infrared Sounder (AIRS) and the Measurement Of Pollution In The Troposphere (MOPITT) satellites FT carbon monoxide trends (2000-2022) also show a peak in ~March-May. Finally, these results demonstrate the need for monthly or seasonally-resolved analyses, as opposed to annual means, for the robust attribution of observed ozone trends.

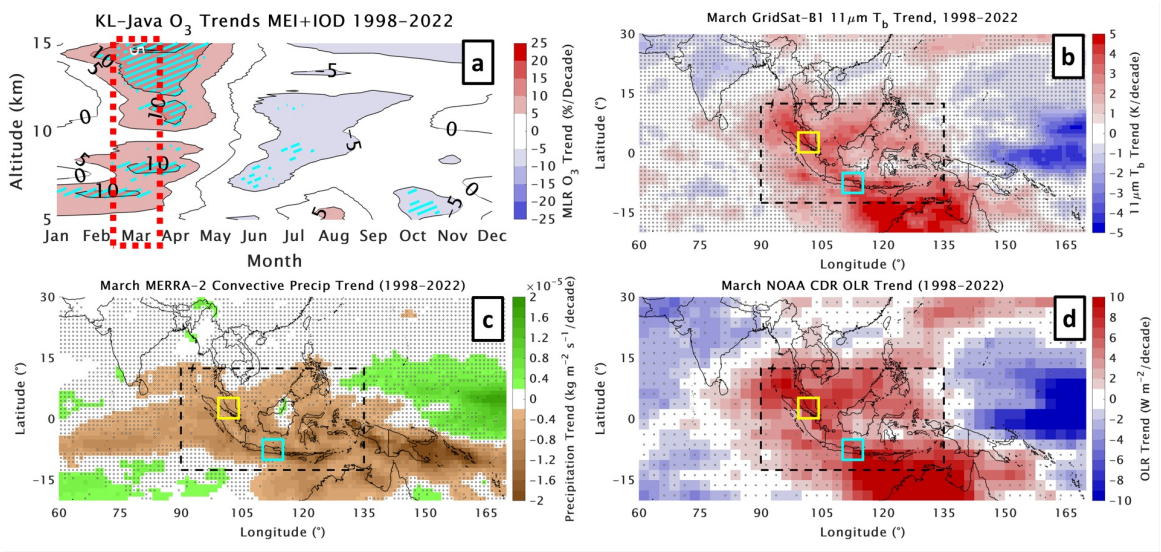

Figure 1. (a): Multiple linear regression FT ozone trends in percent per decade from 5-15 km (cyan hatching indicates 2-sigma statistical significance) from merged Kuala Lumpur-Watukosek (KL-Java) SHADOZ data. The month of March (*see panels b-d*) is highlighted by the red dashed box. (b): March GridSat-B1 11 micron IR brightness temperature (T_b) trends in K per decade. (c): March Modern-Era Retrospective analysis for Research and Applications (MERRA)-2 convective precipitation trends in kg m^{-2} s^{-1} per decade. (d) March outgoing longwave radiation (OLR) trends in W m^{-2} per decade. All panels show trends for 1998-2022. Stippling on panels b-d indicate *insignificant* trends. Yellow (Kuala Lumpur), blue (Watukosek), and black boxes on the panel b-d maps represent regions for which trends will be highlighted in our study.

2021 Wildfires in Siberia as Seen from the TROPOMI: a "Coal Fire" Hypothesis

L. Yurganov

Joint Center for Earth Systems Technology (JCET), University of Maryland, Baltimore County (UMBC), Baltimore, MD 21250; 803-814-2052, E-mail: yurganov@umbc.edu

Wildfire season of 2021 in the Northern Hemisphere was extremely severe. The Atmospheric Infrared Sounder (AIRS)/Aqua data in accordance with the wildfire data base GFED4 evidences record-breaking CO emissions in the Northern hemisphere and, in particular, in Siberia [1], Fig. 1. These wildfires occurred in permafrost and tundra areas of the Central Siberian plateau. Mechanisms of carbonaceous gas emissions still are unknown. Here we analyze the TROPOspheric Monitoring Instruments (TROPOMI) total column CO measurements for this area and compare them with AIRS data.

The TROPOMI is a Short-Wave Infrared (SWIR) imaging spectrometer on board the European Space Agency's Sentinel-5 Precursor (S5-P) satellite that was launched into a sun-synchronous polar orbit in October, 2017. The Royal Netherlands Meteorological Institute (KNMI) and the Netherlands Institute for Space Research (SRON) are responsible for the data processing [2]. An excellent spatial resolution (7.2 × 5.6 km² footprint) and high sensitivity to the lowest troposphere allow to resolve small patches of the burning Earth's surface. Single pixels of CO concentrations averaged over the total atmospheric column (X_{CO}) in early August, 2021 were plotted in a map of Fig. 2. X_{CO}=~500 ppb prevails in the fire zone. Corresponding AIRS data for the same area (not shown here) were in the range 200-250 ppb without any signs of local irregularities. Background X_{CO} for both sounders were well below 100 ppb that was typical for summer time. Relatively small patches with X_{CO} between 650 and 700 ppb were observed. Typical sizes of the "hot spots" varied between single pixels (~6 km) and 5 pixels (~30 km). Some plumes stretched in the direction of the wind for 500 km or more.

The southernmost part of the fire area is characterized by sparse and undersized swampy larch forests. The plateau Putorana with mean height 500-700 m and a maximum of 1,678 m is occupied by mountain tundra or Arctic desert. This area is called the Siberian Traps, it was formed 252 million years ago by one of the largest-known volcanic events of the Earth's geological history. Modern studies assume that the volcanic activity initiated catastrophic combustion of fossil coal. Greenhouse (GH) warming effect of emitted CO_2 and CH_4 was overlapped by sporadic cooling by volcanic aerosol. Irregular and strong climatic changes led to the fact that ~90% of terrestrial and oceanic species were destroyed (the so-called "Permian extinction"). We hypothesize that coal burning explains anomalous emission of GH gases and CO in July-August, 2021.

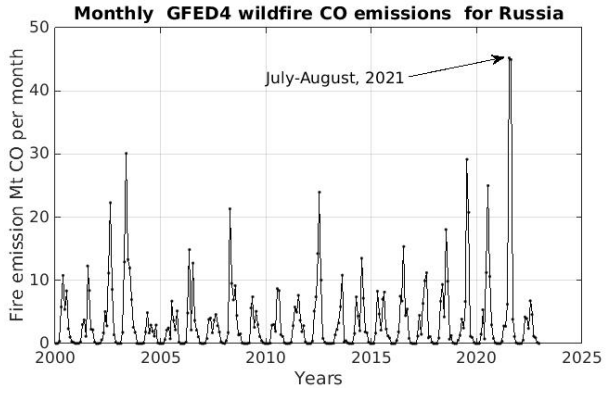

Figure 1. Total monthly CO wildfire emissions from Russia according to the GFED4 database.

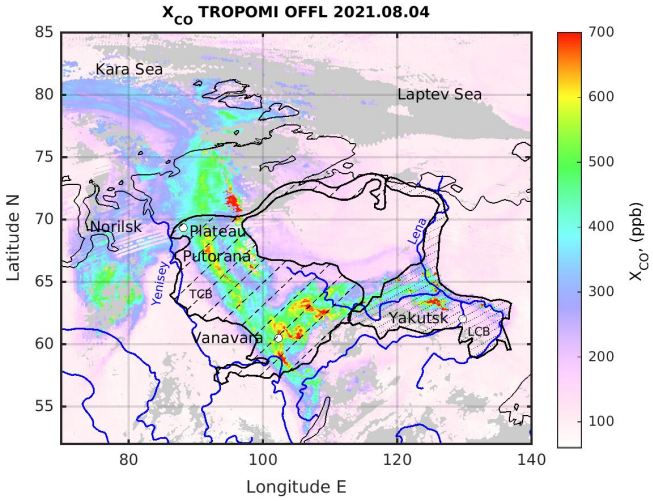

Figure 2. Map of vertically-averaged CO concentration X_{CO}. Hatched areas indicate locations of the world-largest Tunguska Coal Basin (TCB) and Lena Coal Basin (LCB).

Variabilities in Surface Ozone at the Doon Valley of the Himalayan Foothills: Role of Different Chemical Processes

M.C. Rajwar[1,2], M. Naja[1], V. Tomar[1], Y. Kant, and R.K. Tiwari[2]

[1]Aryabhatta Research Institute for observational sciences (ARIES), Department of Science and Technology (DST), Atmospheric Science Division, Govt. of India, Nainital, Uttarakhand, India; +91-972-077-2134, E-mail: mahendar@aries.res.in
[2]Deen Dayal Upadhyaya Gorakhpur University, Gorakhpur, India

South Asia is one of the most diverse regions, home to pristine Himalayan ranges and the most polluted regions, i.e., the Indo-Gangetic Plain (IGP). However, ground-based observations of trace species are highly limited in this region. Because of this, observations of surface ozone have been made at Dehradun (30.330°N, 78.04O°E, 700 a.m.s.l.), a valley site between the Himalayas foothills and the IGP region's proximity from August 2009 to September 2018. Diurnal variations at Dehradun show higher daytime levels than nighttime throughout the year, implying the photochemical production of surface ozone during the daytime. Further, an evening (8.5 ppbv/h) and morning (8.0 ppbv/h) time rate of change of ozone (dO^3/dt) at the site suggests a typical urban environment. A significant monthly variation was observed, with the maximum levels in late springtime (May; 45±15.5 ppbv) and the minimum in the summer/monsoon (July; 15±7.5 ppbv). Sometimes during springtime, the hourly levels exceed 100 ppbv levels, and a secondary maximum is also observed in late autumntime (November; 30±12.4 ppbv). These monthly variations were similar to the other northern Indian (Nainital; Pantnagar) sites. The springtime maxima revealed the role of strong photochemistry in the presence of excessive precursors under the shadow of strong solar radiation with some effect of small-scale dynamic processes. The monthly variation also suggests the influence of boundary level height and biomass burning during spring and autumn at Dehradun. The comparison of monthly surface ozone variability at Dehradun with other Indian subcontinent sites shows the region's heterogeneity in ozone distribution processes. The modeled (CAMs) and observational temporal variabilities are in good agreement at Dehradun except for Summer/Monsoon season, where model results overestimate (20-25 ppbv) the ozone levels than observations. The photochemical production regime of ozone production assesses through the ratio (H_2O_2/HNO_3) analysis for model results. These results are further reconfirmed by other ratio sensitivity indicators ($HCHO/NO_2$). Both hands are in good agreement and suggestion the NO_x-limited regime. A photochemical box model (NCAR-Master Mechanism) was also used to understand the photochemical ozone budget, sensitivity simulation and the role of different NMHC groups at Dehradun and suggest the dominant role of aromatics NMHCs in photochemical ozone production. More details will be presented during the conference.

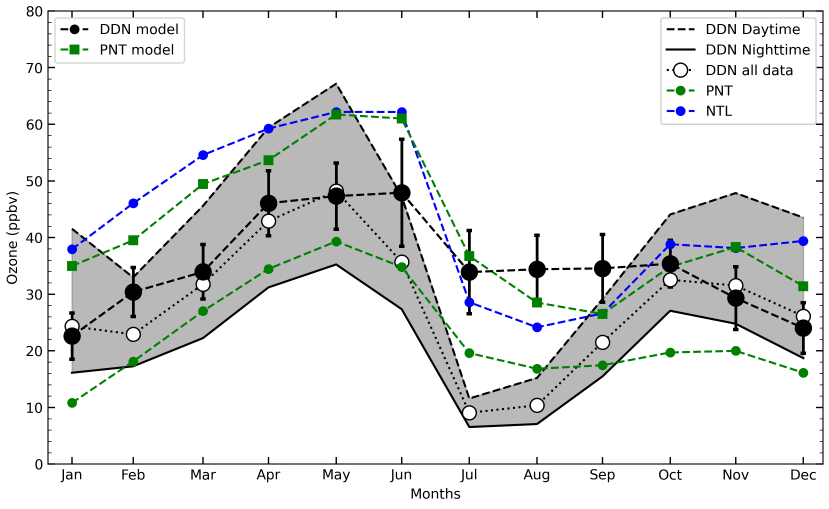

Figure 1. Comparison of Seasonal variations in monthly, daytime (1130–1630 h) and nighttime (0100–0300 h) average ozone at Dehradun with CAMs modeled dataset. Monthly average ozone mixing ratios are also shown at a nearby high-altitude site (Nainital) and a semi-urban site in Pantnagar.

A New Era for Observing Air Quality from Space

G. Frost

NOAA Chemical Sciences Laboratory (CSL), Boulder, CO 80305; 720-767-2174, E-mail: gregory.j.frost@noaa.gov

Until recently, space-based observations of tropospheric air pollutants such as nitrogen dioxide, tropospheric ozone, sulfur dioxide, and formaldehyde have been made by instruments operating in the visible-ultraviolet spectral region on satellite platforms in low Earth orbit, which allows for only one observation per day of any particular location on the globe. A new era began 3 years ago with satellite missions led by South Korea and more recently by the United States that feature instruments measuring these same air pollutants from geostationary orbit, which affords continuous observations of a geographic region during daylit hours. The National Institute of Environmental Research of the Korean Ministry of Environment launched the Geostationary Environmental Monitoring Spectrometer (GEMS) mission onboard the GEO-KOMPSAT 2B in 2020, and the GEMS instrument has been collecting air quality observations over East Asia ever since. The Tropospheric Emissions: Monitoring of Pollution (TEMPO) instrument, NASA's first Earth Venture Instrument mission, was launched on Intelsat 40e in April of this year and will begin measuring air pollution over much of North America and the Caribbean later this summer. NOAA’s plans for its Geostationary Extended Observations mission (GeoXO) include the Atmospheric Composition Instrument (ACX) on GeoXO’s third spacecraft, scheduled for launch in 2036. Highlights of these missions and the applications of their observations to air quality understanding and prediction will be presented.

Remote-Sensing Derived Trends in Gross Primary Production Explain Increases in the CO_2 Seasonal Cycle Amplitude

L. He[1,2], B. Byrne[3], Y. Yin[1], J. Liu[4], and C. Frankenberg[4]

[1]California Institute of Technology, Pasadena, CA 91125; 626-714-9918, E-mail: lhe@carnegiescience.edu
[2]Carnegie Institution for Science, Department of Global Ecology, Stanford, CA 94305
[3]University of Toronto, Toronto, Ontario, Canada
[4]NASA Jet Propulsion Laboratory, California Institute of Technology, Pasadena, CA 91109

An increase in the seasonal cycle amplitude (SCA) of atmospheric carbon dioxide (CO_2) since the 1960s has been observed in the Northern Hemisphere (NH). However, dominant drivers of the amplified CO_2 seasonality are still debated. In this study, we employ satellite-based remote sensing observations to track spatial and temporal changes in global gross primary production (GPP) of different vegetation types. Then, we use a state-of-art atmospheric transport model to examine whether our bottom-up estimates of ecosystem fluxes can capture the magnitude of CO_2 SCA trends at multiple surface sites. Further, we explore dominant drivers of the observed CO_2 SCA trends across different locations of sites. To our best knowledge, this paper makes the first effort to link long-term satellite remote sensing observations with ground atmospheric CO_2 measurements across the NH to explore how terrestrial carbon fluxes shape and change spatiotemporal pattern of atmospheric CO_2.

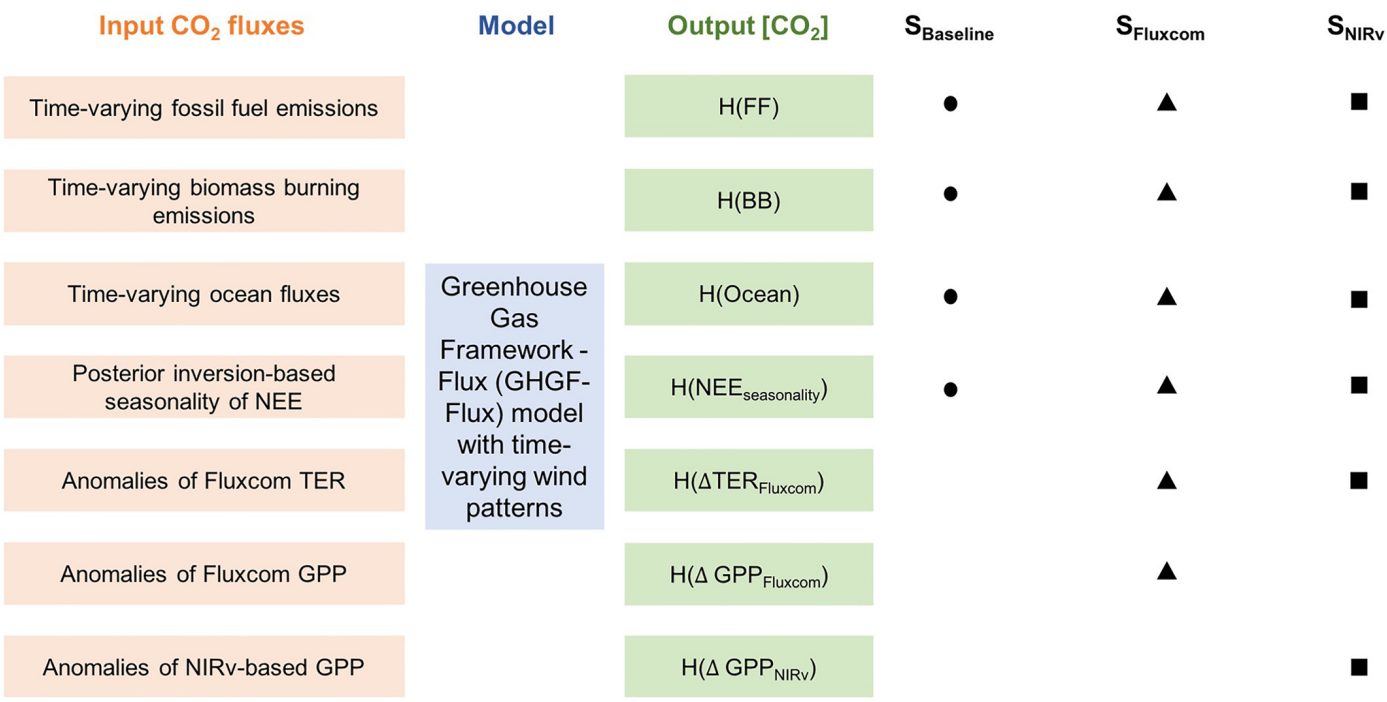

Figure 1. Diagram of the $S_{Baseline}$, $S_{Fluxcom}$, and S_{NIRv} simulations based on CO_2 fluxes from multiple sources. [CO_2] represents the atmospheric CO_2 concentrations. Mathematically, [CO_2] simulated in $S_{Baseline}$, $S_{Fluxcom}$, and S_{NIRv} can be formulated as $H(FF) + H(BB) + H(Ocean) + H(NEE_{seasonality})$, $H(FF) + H(BB) + H(Ocean) + H(NEE_{seasonality}) + H(\Delta TER_{Fluxcom}) + H(\Delta GPP_{Fluxcom})$ and $H(FF) + H(BB) + H(Ocean) + H(NEE_{seasonality}) + H(\Delta TER_{Fluxcom}) + H(\Delta GPP_{NIRv})$, where H(X) denotes the application of a forward atmospheric model to simulate CO_2 concentrations driven by fluxes X.

Developing an Australian Greenhouse Gas Observing Network (AGGON)

C. Caldow[1], R.L. Langenfelds[2], Z. Loh[2], C.M. Trudinger[2], A.R. Stavert[1], P.B. Krummel[2], E. Guerette[2], D.M. Etheridge[2], A.K. Luhar[1], P.J. Fraser[1], B. Mitrevski[2], C. Roulston[1], J. Ramirez-Gamboa[1], N. Shahrokhi[1], B. Dunse[2], T. Ziehn[1], and R.M. Law[1]

[1]Commonwealth Scientific & Industrial Research Organisation (CSIRO), Aspendale, VIC 3195, Australia; 029-239-4404, E-mail: christopher.caldow@csiro.au
[2]Commonwealth Scientific and Industrial Research Organisation (CSIRO), Oceans and Atmosphere, Aspendale, Victoria, Australia

The Paris Agreement has been signed by 195 parties who together account for more than 95% of global greenhouse gas (GHG) emissions. Yet based on current emissions, we're likely to deplete the remaining carbon budget within the next 10 or 30 years, to increase global average temperatures by 1.5 °C or 2 °C above pre-industrial levels, respectively (Friedlingstein et al. 2022; Liu et al. 2023). Whilst global emissions continue to rise, more than 70 countries now have net zero targets, covering about 76% of global emissions (UN, 2022). Trillions of dollars have already been allocated and invested to reach net zero, with the total amount required estimated in the hundreds of trillions of dollars (IEA 2021; Kumra & Woetzel 2022; United Nations Framework Convention on Climate Change (UNFCCC), 2021). The effectiveness of greenhouse gas mitigation strategies, including the targeting of investment, relies heavily on the accuracy of greenhouse gas accounts. It is therefore essential that these accounts are informed by the most up-to-date science.

Australia's National Greenhouse Accounts are used to meet emissions reporting requirements under the Paris Agreement, UNFCCC and Kyoto Protocol. These accounts are almost exclusively compiled using 'bottom-up' methods, which have been shown to contain significant uncertainty and may not account for potentially large sources (Assan et al. 2022; Dunse et al. 2022; Luhar et al. 2020; Neininger et al. 2021; Sadavarte et al. 2021). Where 'top-down' methods have been applied, they have provided invaluable independent assessment of the accuracy of emissions and methodologies included in the national accounts, as well as insights that can be used to improve the national accounts (DISER 2021; 2022). It is for reasons such as these, that IPCC emissions reporting guidelines were revised in 2019 to encourage greater use of top-down methods, and that the WMO have recently proposed an expanded global GHG monitoring system (IPCC 2019; WMO 2023).

The Australian atmospheric science community has established expertise in GHG measurements and inverse modelling of fluxes, and a proven track record in applying top-down methods on global, regional and local scales. However, contributions to national emissions verification are presently limited by sparsity of observations, with only 4 long-term sites covering an area comparable to either Europe or the USA (Figure 1) resulting in a relatively high reliance on satellite and short-term (campaign-based) observations.This presentation will provide an overview of recent and continuing efforts to expand the Australian Greenhouse Gas Observation Network (AGGON) including network design, instrumentation, and resourcing requirements.

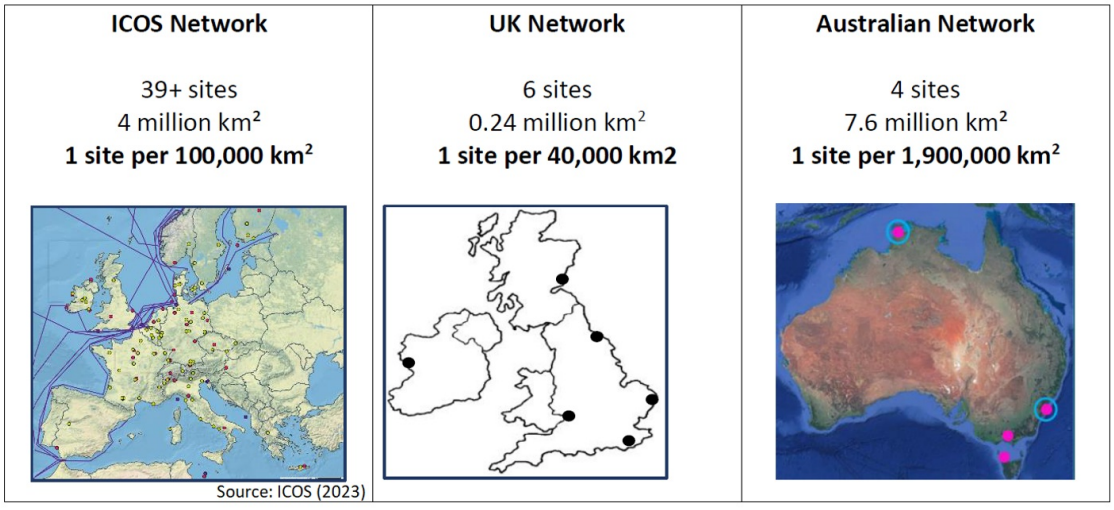

Figure 1. *Map of atmospheric GHG monitoring networks for Europe (ICOS), the United Kingdom and Australia showing the number of sites relative to land surface area.*

Evaluation of the Impact of the Expanded *in Situ* Measurement Network on the Diagnosis of North American Methane Fluxes

N. Miles[1], D. Wesloh[1], Y. Cui[1], S. Feng[1], A. Andrews[2], L. Hu[2], K. Thonig[2], S. Prinzivalli[3], W. Callahan[3], J. Marlow[1], and K.J. Davis[1,4]

[1]The Pennsylvania State University, Department of Meteorology and Atmospheric Science, University Park, PA 16802; 814-880-8087, E-mail: nmiles@psu.edu
[2]NOAA Global Monitoring Laboratory (GML), Boulder, CO 80305
[3]Earth Networks, Inc., Germantown, MD 20876
[4]Earth and Environmental Systems Institute, The Pennsylvania State University, University Park, PA 16802

Accurate diagnosis of methane (CH_4) emissions at regional scales is crucial in order to monitor progress towards emissions reductions attributable to policy changes. In this study, we use the regional inversion system CarbonTracker-Lagrange (CT-L) to diagnose North American methane emissions to evaluate the impact of the increasing density of the in-situ tower-based measurement network. We show results from an ensemble of six priors and four measurement networks, for seven regions within the North American domain. The posterior indicates an increase in emissions above the most realistic prior for six of the seven regions, with the most dramatic difference being in the central region of the U.S.. The differences in the regional totals using the different measurement networks are small (0.3-15.4% in magnitude, except for the western U.S. region), even starting from a spatially flat prior. Additional towers included in the inversion increase the error reduction slightly from 63% to 69% for the continental total. Using the most dense tower network available, the normalized standard deviation of the posteriors using multiple priors is reduced substantially for much of the U.S. (from 11% to 5% in the midwest, for example). We cross evaluate the inverse flux estimates using independent atmospheric CH_4 mole fraction observations from the Atmospheric Carbon and Transport (ACT) - America Earth Venture Suborbital flight campaigns, finding that the enhanced network improves agreement in the northeast U.S., from a bias of 10.4 ppb for the minimal network to 3.8 ppb. We conclude that even a relatively sparse tower network is able to infer the large-scale patterns and net fluxes of methane from North America. Increased network density does increase the resolution of the inversion system and reduces biases, and thus is beneficial for understanding regional, seasonal-scale methane emissions.

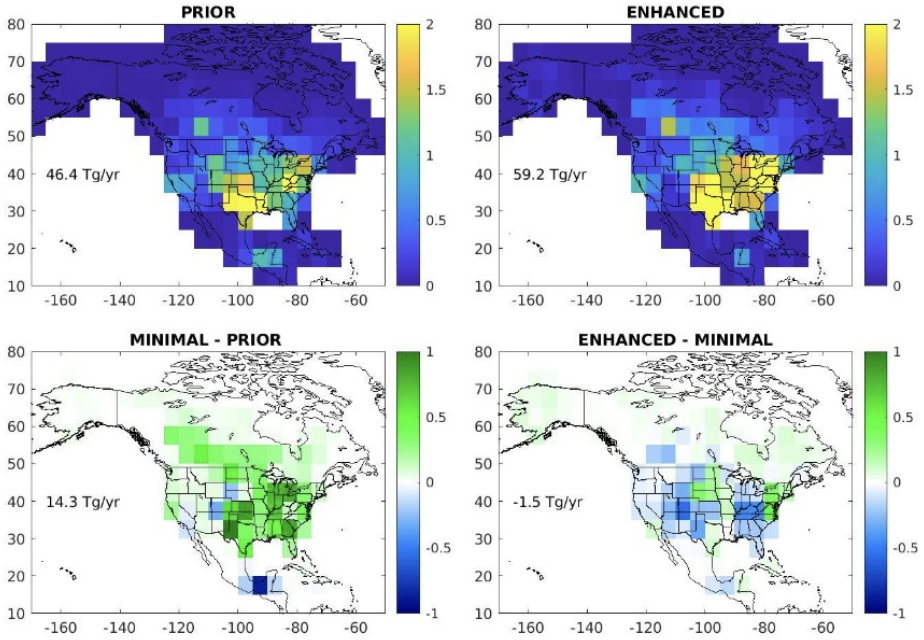

Figure 1. Prior emissions, posterior emissions using the enhanced network, difference from the prior for the minimal network posterior, and difference between enhanced and minimal network posteriors. Units are Tg/yr/5°x5° pixel.

Identifying Methane Emissions from Animal Feeding Operations in a Mixed Emission Region Within the Colorado Front Range

K.M. Steinmann[1], M.E. McCabe[1], J.F.J. Calahorrano[2], A. Sullivan[2], I.B. Pollack[2], E.V. Fischer[2], and D.R. Caulton[1]

[1]University of Wyoming, Laramie, WY 82071; 307-766-3245, E-mail: ksteinma@uwyo.edu
[2]Colorado State University, Department of Atmospheric Science, Fort Collins, CO 80523

Agriculture and oil and natural gas (ONG) production are two of the largest sources of methane (CH_4) emissions in the U.S and are often found near each other, like in the northern Colorado Front Range (NCFR), making CH_4 source attribution difficult. Using data from the Transport and Transformation of Ammonia (TRANS^{2}Am) campaign, we separate CH_4 emissions related to agriculture from other sources, like ONG production. Phase one of the TRANS^{2}Am campaign consisted of 15 research flights during August 2021 over the NCFR (Figure 1 shows the flight path for RF 13). CH_4, ammonia (NH_3), and ethane (C_2H_6) concentrations were measured using the University of Wyoming King Air (UWKA) research aircraft, which circled concentrated animal feeding operations (CAFOs) housing sizable beef and dairy cattle populations. Two different approaches were used to differentiate CH_4 emissions by source. The first approach removed the CH_4 associated with ONG by subtracting an amount of CH_4 based on the C_2H_6:CH_4 ratio. The second approach estimates the CH_4 emissions from CAFOs using multivariate regression (MVR), incorporating the NH_3 concentration and NH_3:CH_4 ratio. These two approaches were used to calculate CH_4 emissions from CAFOs sampled during the first phase of the TRANS^{2}Am campaign. We have found that our calculated CAFO CH_4 emissions are slightly higher than those of previous studies and the EPA's National Emission Inventory estimate for beef cattle. This research shows the importance of correctly attributing CH_4 emission sources to properly represent CH_4 sources in inventories and to better understand the role of livestock emissions on the atmosphere and climate.

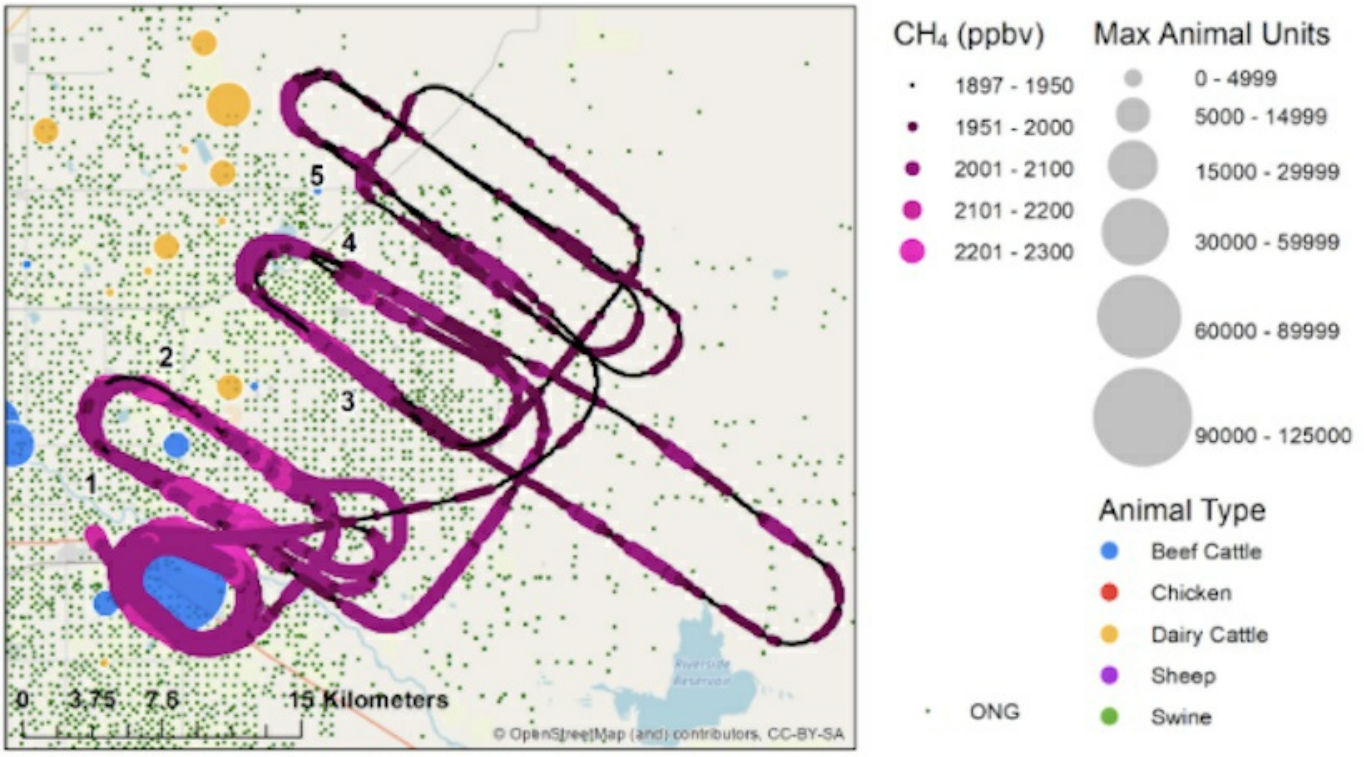

Figure 1. Path of TRANS^{2}Am RF 13, colored by CH_4 (ppbv). Black numbers represent the corresponding transect number. Animal operations are indicated by the different colored circles as in Figure 1. Green dots represent ONG wells, data of ONG as of 2015 (Colorado Department of Natural Resources Oil & Gas Conservation Commission).

Updated Time-varying Maps of Surface Ocean $\delta^{13}C$ of DIC and the $^{13}CO_2$ Isotopic Disequilibrium Flux with Uncertainty

D. Munro[1,2], J.B. Miller[2], A. Fay[3], and P.D. Quay[4]

[1]Cooperative Institute for Research in Environmental Sciences (CIRES), University of Colorado, Boulder, CO 80309; 303-497-5765, E-mail: david.munro@noaa.gov
[2]NOAA Global Monitoring Laboratory (GML), Boulder, CO 80305
[3]Department of Earth and Environmental Sciences, Columbia University and Lamont Doherty Earth Observatory
[4]University of Washington, Seattle, WA 98105

Estimates of spatial and temporal patterns in the ^{13}C:^{12}C ratio (expressed as $\delta^{13}C$) of surface ocean dissolved inorganic carbon (DIC) are essential for interpreting atmospheric $\delta^{13}C$ of CO_2. The work described here is part of a larger project focused on using atmospheric CO_2 and $\delta^{13}C$ measurements to quantify terrestrial and oceanic net carbon fluxes as well as isotopic fractionation by terrestrial plants. Previously, we compiled a dataset of more than 8700 surface ocean $\delta^{13}C$ of DIC measurements collected from research vessels and ships of opportunity from 1978 to 2018. In this analysis, we use a trend analysis over different regions of the global oceans and the approach of Takahashi et al. [2009] to create monthly maps of $\delta^{13}C$ of DIC on a 4˚ (latitude) x 5˚ (longitude) spatial grid from 1990 to 2021. These values are then used to calculate the ^{13}C isotopic disequilibrium flux at the same spatial and temporal resolution. The uncertainty of the $\delta^{13}C$ of DIC is estimated using cross-validation whereby surface ocean $\delta^{13}C$ of DIC observations are withheld and then compared to gridded predictions. We then use the cross-validation statistics to inform a Monte Carlo scheme to estimate the uncertainty of ^{13}C isotopic disequilibrium flux for each grid cell. We use the same Monte Carlo scheme to assess the uncertainty of both the gross and net air-sea CO_2 flux from 1990 to 2021 and compare this uncertainty to the spread of estimates based on widely-available surface ocean partial pressure of CO_2 (pCO_2) products covering the same time interval. We find that uncertainties related to air-sea gas exchange can be substantial relative to the spread among estimates due only to differences in the pCO_2 product used in the flux estimate.

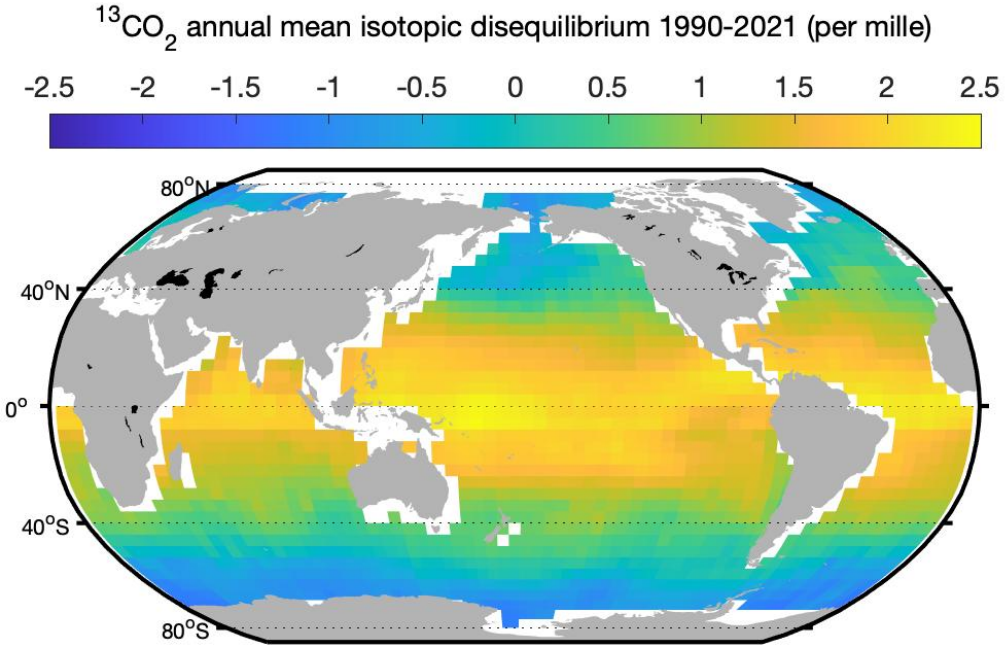

Figure 1. Fig. 1. Annual mean $^{13}CO_2$ isotopic disequilibrium in per mille for 1990-2021.